

Extraction of Nonlinear Hysteretic Properties of Seismically Isolated Bridges from Quick-Release Field Tests

by

Qingbin Chen, Bruce M. Douglas,
Emmanuel Maragakis and Ian G. Buckle
Center for Civil Engineering Earthquake Research
University of Nevada at Reno
University Station
Reno, Nevada 89507-8121

Technical Report MCEER-98-0001

May 26, 1998

This research was conducted at the University of Nevada, Reno and was supported by the Federal Highway Administration under contract number DTFH61-92-C-00106.

NOTICE

This report was prepared by the University of Nevada, Reno as a result of research sponsored by the Multidisciplinary Center for Earthquake Engineering Research (MCEER) through a contract from the Federal Highway Administration. Neither MCEER, associates of MCEER, its sponsors, the University of Nevada at Reno, nor any person acting on their behalf:

- a. makes any warranty, express or implied, with respect to the use of any information, apparatus, method, or process disclosed in this report or that such use may not infringe upon privately owned rights;
or
- b. assumes any liabilities of whatsoever kind with respect to the use of, or the damage resulting from the use of, any information, apparatus, method, or process disclosed in this report.

Any opinions, findings, and conclusions or recommendations expressed in this publication are those of the author(s) and do not necessarily reflect the views of MCEER or the Federal Highway Administration.

Extraction of Nonlinear Hysteretic Properties of Seismically Isolated Bridges from Quick-Release Field Tests

by

Q. Chen¹, B.M. Douglas², E.M. Maragakis³, and I.G. Buckle⁴

Publication Date: May 26, 1998

Submittal Date: June 30, 1997

Technical Report MCEER-98-0001

Task Number 106-F-4.3.1(b)

FHWA Contract Number DTFH61-92-C-00106

- 1 Research Assistant, Department of Civil Engineering, University of Nevada, Reno
- 2 Director and Professor, Center for Civil Engineering Earthquake Research, Department of Civil Engineering, University of Nevada, Reno
- 3 Chairman and Professor, Department of Civil Engineering, University of Nevada, Reno
- 4 Deputy Vice Chancellor, Research, The University of Auckland, Auckland, New Zealand

MULTIDISCIPLINARY CENTER FOR EARTHQUAKE ENGINEERING RESEARCH
State University of New York at Buffalo
Red Jacket Quadrangle, Buffalo, NY 14261

Preface

The Multidisciplinary Center for Earthquake Engineering Research (MCEER) is a national center of excellence in advanced technology applications that is dedicated to the reduction of earthquake losses nationwide. Headquartered at the State University of New York at Buffalo, the Center was originally established by the National Science Foundation in 1986, as the National Center for Earthquake Engineering Research (NCEER).

Comprising a consortium of researchers from numerous disciplines and institutions throughout the United States, the Center's mission is to reduce earthquake losses through research and the application of advanced technologies that improve engineering, pre-earthquake planning and post-earthquake recovery strategies. Toward this end, the Center coordinates a nationwide program of multidisciplinary team research, education and outreach activities.

MCEER's research is conducted under the sponsorship of two major federal agencies, the National Science Foundation (NSF) and the Federal Highway Administration (FHWA), and the State of New York. Significant support is also derived from the Federal Emergency Management Agency (FEMA), other state governments, academic institutions, foreign governments and private industry.

The Center's FHWA-sponsored Highway Project develops retrofit and evaluation methodologies for existing bridges and other highway structures (including tunnels, retaining structures, slopes, culverts, and pavements), and improved seismic design criteria and procedures for bridges and other highway structures. Specifically, tasks are being conducted to:

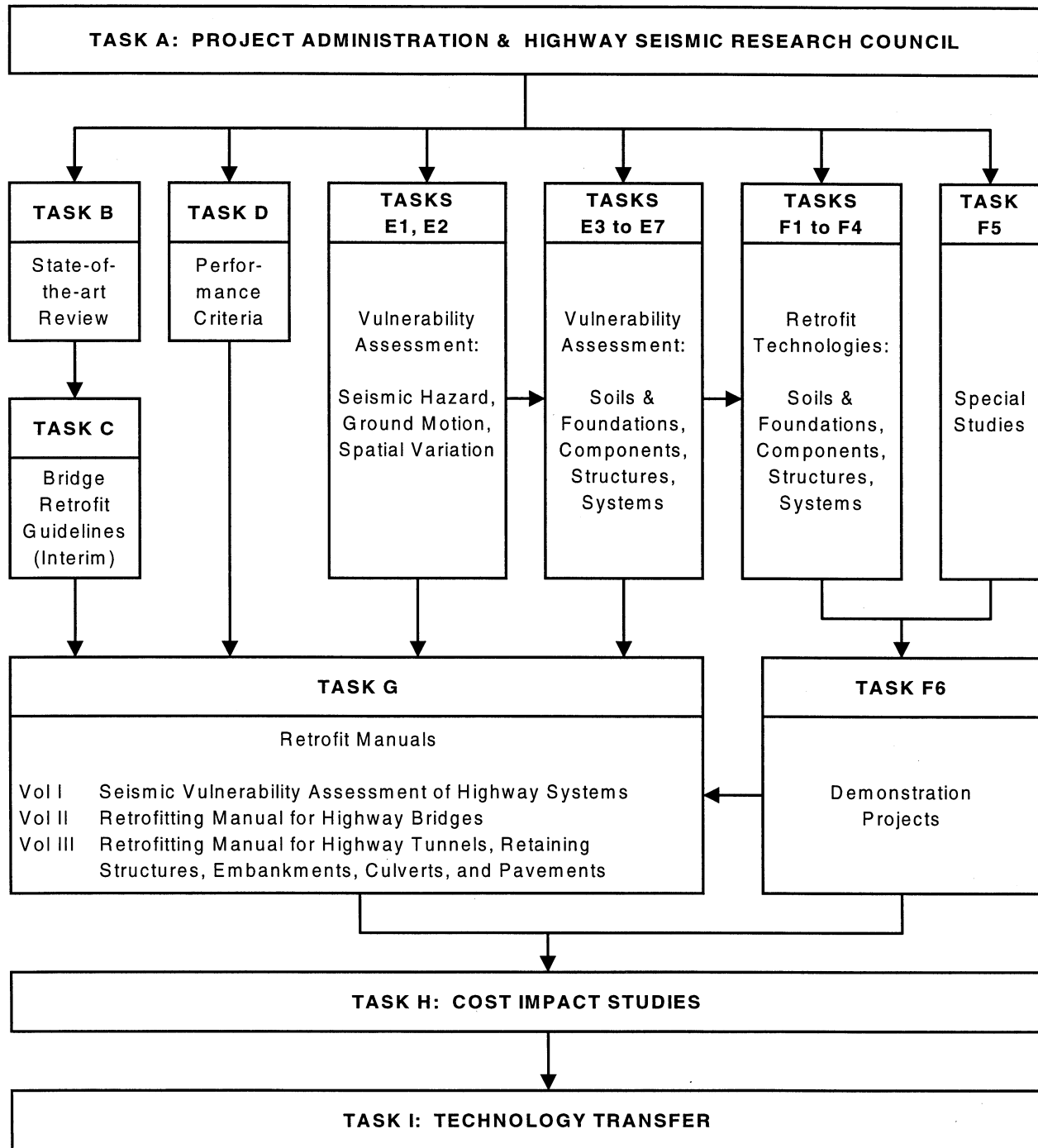
- assess the vulnerability of highway systems, structures and components;
- develop concepts for retrofitting vulnerable highway structures and components;
- develop improved design and analysis methodologies for bridges, tunnels, and retaining structures, which include consideration of soil-structure interaction mechanisms and their influence on structural response;
- review and recommend improved seismic design and performance criteria for new highway structures.

Highway Project research focuses on two distinct areas: the development of improved design criteria and philosophies for new or future highway construction, and the development of improved analysis and retrofitting methodologies for existing highway systems and structures. The research discussed in this report is a result of work conducted under the existing highway structures project, and was performed within Task 106-F-4.3.1(b), "Field Testing of a Seismically Isolated Bridge" of that project as shown in the flowchart on the following page.

The overall objective of this task was to develop nonlinear models for use in seismic vulnerability assessments of isolated bridges. The report describes the development of an optimized procedure to perform such an assessment. To develop the procedure, the authors first identified the properties of interest of the seismic isolators, then modeled the hysteretic characteristics of the bridge-isolator system. An analytical solution for the response of a bilinear SDOF system to

quick-release excitation was derived. Data from two different quick-release tests were used to test the procedure. The predicted vs. observed test data were compared and showed good agreement. Thus, the authors concluded that quick-release field test data could be successfully used to extract nonlinear hysteretic properties of seismically isolated bridges.

SEISMIC VULNERABILITY OF EXISTING HIGHWAY CONSTRUCTION
FHWA Contract DTFH61-92-C-00106



ABSTRACT

A time domain system identification method is used to identify the hysteretic properties of lead-rubber bearings installed in seismically isolated bridge systems. The longitudinal or transverse motion of the superstructure is idealized as a single degree of freedom (SDOF) system, where the total damping effect has been divided into two parts.

The most significant component of damping, which is caused by hysteretic behavior, is described directly by the nonlinear models. The viscous damping component, which is assumed to be proportional to the velocity of the mass, is described by the damping ratio.

Two theoretical models are used for modeling the force-displacement characteristics of the rubber-lead bearings. These are the generalized Ramberg-Osgood model and the bilinear model.

A closed form solution for the response of a bilinear SDOF oscillator to quick release excitation was derived and a step by step integration method is used for computing the displacement, velocity and acceleration time histories of the nonlinear SDOF system numerically. The displacement and acceleration time histories of the superstructure observed during quick release tests are compared with theoretical ones in order to identify the important characteristics of the lead-rubber bearings from field experiments.

Time histories recorded from field quick-release tests on two bridges are used for the examples

presented herein. It is shown that this is a simple and efficient method to interpret the data from quick-release field tests. The essential in-situ hysteretic characteristics of lead-rubber isolation bearings can be obtained using this method.

ACKNOWLEDGMENT

We would like to thank Dr. Ian Aiken at the University of California, Berkeley, and Dr. Stuart Chen of the State University of New York at Buffalo for their help in supplying the field data used in this study. We also would like to thank an anonymous reviewer for several very helpful suggestions. The study was funded by the National Center for Earthquake Engineering Research.

TABLE OF CONTENTS

SECTION	TITLE	PAGE
1	INTRODUCTION	1
2	METHODOLOGY	7
3	ANALYTICAL SOLUTION FOR SDOF SYSTEM WITH A BILINEAR HYSTERETIC SPRING	9
3.1	General	9
3.2	Analytical Solution for Zero Damping Case	11
3.3	Analytical Solution for Damped Case	13
4	A GENERALIZED RAMBERG-OSGOOD MODEL AND ITS IMPLIED BILINEAR MODEL	19
4.1	Generalized Ramberg-Osgood Model	19
4.2	Implied Bilinear Model	20
5	IDENTIFICATION OF DYNAMIC PROPERTIES OF SEISMICALLY ISOLATED BRIDGES FROM THE QUICK-RELEASE TIME HISTORIES	25
5.1	Modeling for the Optimization Problem	25
5.2	Numerical Procedure	26
5.3	Parameter Identification Using Data from Full Scale Quick-Release Tests Conducted by University of California at Berkeley	29
5.4	Parameter Identification Using Data from State University of New York at Buffalo	36
6	CONCLUSIONS	47
7	REFERENCES	49

LIST OF ILLUSTRATIONS

FIGURE	TITLE	PAGE
3-1	Bilinear Model	10
3-2	Relation Between α_0 and β for producing Zero Permanent Displacement	16
4-1	Generalized Ramberg-Osgood Model and Its Implied Bilinear Model	21
4-2	Definition of Generalized Ramberg-Osgood Model	22
4-3	Comparison between the Hysteretic Model and Experimental Data	23
5-1	An Example for Parameter Identification	28
5-2	A Sketch of the Seismically Isolated Viaduct in Walnut Creek, California	30
5-3	Time Histories of Quick-Release Test Conducted by the University of California at Berkeley	31
5-4	Optimization Results Using Generalized Ramberg-Osgood Model and the Quick-Release Testing Data from UC Berkeley	32
5-5	Optimization Results Using Bilinear Model and the Quick-Release Testing Data from UC Berkeley	33
5-6	Force Displacement Views for Bearing Tests and Optimization Results	34
5-7	Plan and Side View of Cazenovia Creek Bridge in New York State	37
5-8	Acceleration and Displacement Time histories Measured at the North Pier	38
5-9	Acceleration and Displacement Time histories Measured at the South Pier	39
5-10	Averaged Time Histories for the North and South Piers	40
5-11	Optimization Results Using the Generalized Ramberg-Osgood Model and the Quick-Release Testing Data from SUNY at Buffalo	41
5-12	Optimization Results Using Bilinear Model and the Quick-Release Testing Data from SUNY at Buffalo	42
5-13	Comparison the Hysteretic Loops Between the Optimization Results and Laboratory Tests	45

LIST OF TABLES

TABLE	TITLE	PAGE
5-1	Summary of the Optimization Results Using UC Berkeley's Quick-Release Testing Data	35
5-2	Summary of the Optimization Results Using NCEER's Quick-Release Testing Data	44

SECTION 1

INTRODUCTION

A notable change in conventional seismic design methods in past years has been the introduction of the concept of ductility. The main purpose for introducing ductile elements in structures is to absorb energy, thus avoiding collapse during major earthquakes. These highly yielded structures, however, may not necessarily be repairable. A challenging task today is to find practical design technologies which protect both life and structure with a minimum extra cost. Among the efforts toward this goal, seismic isolation is one of the most promising concepts.

Seismic isolation is a passive seismic control technology which has developed rapidly in recent years (Buckle et. al., 1990). The goal of reducing earthquake induced forces in isolated structures is attained by introducing bearings, which are very flexible in the horizontal direction, between the base of the structure and the foundation. The flexible bearings change the dynamic characteristics of the structures in three ways. First, the fundamental frequency of the structure is reduced so that it is much lower than the predominant frequency of the strong ground motion. Second, the flexible bearings provide a special mode shape in which the distribution of the shear distortions are concentrated in the bearings rather than distributed throughout the entire structure. The main structure benefits from this special mode shape by reducing the overall shear forces in it. Third, the resonant displacement associated with the fundamental isolation mode can be significantly reduced by introducing a damping mechanism in the bearings.

The motion of higher modes in superstructures may not benefit from the damping of the bearings. However, according to the linear model proposed by Kelly (1990), the higher modes are “highly decoupled” from the high frequencies of earthquake ground motions. In bridge engineering, seismic isolation is becoming an economic and efficient alternative to conventional design in protecting the columns and superstructures from damage (Mayes, et al., 1992). Some successful examples of the use of seismic isolation technology have been observed in Japan and the United States during the Kobe and Northridge earthquakes. (Moehle, 1994, Asher et al., 1997). In the retrofitting process,

the supports are replaced by bearings made with special materials. One type of isolation bearing is made of laminated rubber having a lead core. The basic characteristic of this type of bearing is that it has a substantial stiffness in the vertical direction to carry the dead loads and a relatively small shearing stiffness, which shifts the fundamental period in the structure.

The practice of seismic isolation concepts began in the 1970's in New Zealand (McKay, 1990). Other work on this concept was conducted in Japan, Italy, France, Greece and China (Buckle et al., 1990, Kelly, 1986). In the United States, a major factor for limiting the use of this technology was the lack of a suitable code (Mayes, et al. 1992). As a key step, in 1991, AASHTO published a guide specification for seismic isolation design (AASHTO, 1991). In the AASHTO design procedure, the energy dissipation of the isolation system is expressed in terms of an equivalent viscous damping, and the stiffness was expressed as an effective linear stiffness. The dynamic behavior of seismically isolated structures is controlled by the hysteretic properties of the isolators, and is strongly nonlinear. Starting in 1976 at the Earthquake Engineering Research Center at University of California at Berkeley, a series of the theoretical and laboratory studies for the force-displacement behavior of elastomeric rubber bearing were carried out (Kelly, 1981, 1987, Chen, et al, 1993).

The hysteretic characteristics of lead-rubber isolators have often been represented by a bilinear model for the sake of simplicity. However, laboratory tests have shown that for strains of less than about 100%, when the strain increases, the shear stiffness decreases in a smooth continuous manner; but at larger strains, the shear stiffness begins to increase again. For the purposes of quick-release testing, it is not anticipated that strains much greater than 100% will be required. In this strain range, the generalized Ramberg-Osgood model proposed by Desai (1976) was found to be a more accurate way of representing the hysteretic behavior of lead-rubber bearings. The generalized Ramberg-Osgood model allows for a finite stiffness for large strains, while the backbone curve of the standard Ramberg-Osgood model has a zero stiffness at large strains. Another convenient feature of the generalized Ramberg-Osgood model is the fact that it can also be used to represent a bilinear hysteretic model by choosing the power parameter to be large. Thus, the same basic hysteretic rule can be used for both models within a computer program. It should also be noted that designers can

construct an equivalent bilinear model to describe the bearing behavior once the generalized Ramberg-Osgood parameters have been defined for the particular case in question.

The dynamic characteristics of the lead-rubber bearings depend on many factors such as temperature, aging and loads on the bearings. In the laboratory, only individual bearings can be tested. Dynamic tests are difficult because of their large size. Different types of rubber bearings may be installed on one bridge. The dynamic behavior of a bridge in-situ will be determined by the combined characteristics of all the bearings installed in the bridge. Full scale quick-release tests provide a practical way to obtain the dynamic properties of the entire bearing assemblage. The nonlinear response can be obtained by pulling the structure past the yielding point. Since 1990, several full scale quick-release tests on the highway bridges have been conducted in the United States (Douglas, et. al., 1990, Gilani, et. al., 1995, and Wendichansky, 1996). The time histories from quick release tests contain much information about the dynamic properties of the superstructures, bearings, columns, and foundations. For seismically isolated bridges, however, the major interest is to obtain the nonlinear properties of the isolators.

The important question is how to extract the physical parameters of the rubber bearings from the quick-release time histories. For this purpose, we propose an iterative optimization procedure to obtain the optimal parameters of the generalized Ramberg-Osgood model as well as the damping ratio by fitting the calculated time histories to those obtained from the quick-release tests. We assume that the motion of superstructure can be simulated by a single degree freedom (SDOF) system. In the quick-release test, the bridge is usually pulled and then released in either the longitudinal or the transverse direction. Several conditions are required for the SDOF model to be a valid assumption. The twisting component of motion of the superstructure should be negligible. The data should be dominated by the motion of the fundamental mode, or at least, the motion for the fundamental mode must be separable from the higher mode motions. For purposes of identifying the properties of the isolators, the flexural deformation of the substructure should be small.

In modeling the hysteretic characteristics of the bridge-isolator system, two models were used. The

generalized Ramberg-Osgood model was found to be a flexible and adequate model for representing the hysteretic characteristics of the rubber-lead bearings if the strains in the bearings are not larger than 100%. On the other hand, the simple bilinear model is a very useful equivalent model for analysis and design purposes. Using a step by step numerical method, the nonlinear response of the SDOF system was computed using the generalized Ramberg-Osgood hysteretic rules. For numerical purposes, the generalized Ramberg-Osgood formulation can be made to solve the bilinear hysteretic case with a suitable adjustment of the Ramberg-Osgood parameters. To find the hysteretic properties of a seismically isolated bridge, an objective function was defined as the sum of the squares of the differences between the computed time histories and the observed data, where both the displacement and the acceleration time histories were used in the objective function. A direct search algorithm proposed by Hooke and Jeeves (Hooke and Jeeves, 1961) was used to find the optimal solution, which is defined as the solution which causes the objective function to have a global minimum. Experience has shown that this is a simple, reasonably efficient method to minimize the objective function (Vrontinos, 1994).

An analytical solution for the response of the bilinear SDOF system to quick-release excitation was also derived. This solution is helpful for a better understanding of the behavior of a bilinear SDOF oscillator. For example, the time at which the first yield point is reached after quick release, and the time at which the oscillator returns to the initial stiffness can be calculated theoretically. It can also be shown that significant nonlinear behavior such as the post yielding stiffness and the yield point are contained in the first cycle of the time histories. These theoretical times can guide us in choosing the analysis time window. In quick-release tests, it is desirable to produce as small a permanent displacement as possible. Another useful result is that the initial release displacement required to cause a zero permanent displacement can be found. This is a closed form equation for the case when the damping ratio is zero. For the nonzero damping case, this information can only be obtained from a numerical solution. It was found that the release displacement which causes a zero permanent displacement is sensitive to the damping ratio. Due to the damping effect, larger release displacements are required to cause a zero final displacement than the non-damping case. The analytical solution can also be used to check the correctness of the computer code for the numerical

method.

In order to consider practical examples, two data sets from quick-release field tests were used to find the optimal parameters representing the hysteretic characteristics of rubber-lead bearings. One set is from the full scale quick-release tests carried out by the University of California at Berkeley (Gilani et al., 1995), and another is the quick-release test conducted by the State University of New York at Buffalo (Wendichansky, 1996). The hysteretic curves predicted by the optimized model parameters using this field data were compared directly with the load-displacement data obtained from laboratory tests on the same bearings. It was found that there was no significant disagreement between these results. The result indicates that the optimization procedure proposed in this report is a practical method for analyzing the data from quick-release tests.

SECTION 2 METHODOLOGY

There are two different ways to model the quick-release response of seismically isolated bridges. One is to establish a detailed finite element multiple degree of freedom model, from which the vibration of the entire system can be studied. This detailed model would include the rigid body motion as well as the detailed behavior of the individual structural elements. Another way is to utilize the features of the seismically isolated bridge to establish a simple SDOF model. One of the important characteristics of seismically isolated bridges is that the shearing stiffness of the lead-rubber bearings is significantly lower than the superstructure and columns. In quick release tests, the major deformation occurs in the lead-rubber bearings only. The superstructure behaves almost as a rigid body. For the quick-release test, the bridge is usually pulled and then released in either the longitudinal or transverse direction. By careful design of the load application details, the twisting component of the motion can be reduced to a negligible level. Thus, a single degree of freedom (SDOF) model is suitable for this case. Based on a SDOF model, we propose a system identification method for identifying the hysteretic properties of lead-rubber bearings installed in seismically isolated bridges.

Typically, the displacement time histories for the isolated superstructure obtained in quick-release tests contains two parts. The first cycle, which is dominated by the nonlinear response is the first part. The second part consists of the decaying damped elastic oscillations. The decay of the elastic oscillations implies a viscous damping mechanism. Thus, we assume that the total damping is caused by both hysteretic and viscous damping. The hysteretic damping is described directly by the hysteric force-displacement model. The viscous damping is represented by introducing the velocity proportional term in the equation of motion for the SDOF model.

The displacement time history is usually dominated by fundamental mode. The experimental acceleration time histories, however, may contain the motion of the higher modes. The high frequency motions in the acceleration time histories are excited by the quick-release system. For

longitudinal quick-release tests, the accelerogram may have a large component associated with the signal having a period equal to the time it takes for a wave to travel from one end of the superstructure and reflect back. These high frequency signals might be reduced by designing a quieter release system. For superstructures released transversely, the frequency related to the wave traveling across the width of the deck is too high to be of concern. However, the mode related to the flexural vibration of the superstructure may be dominant in the acceleration time histories. To reduce the motion of the flexural vibration mode, it is better to pull and release the superstructure at multiple points to keep the static release deformation shape as close to the rigid body deformation shape as possible. Our interest is to extract the information for the hysteretic physical properties of the isolators which is contained in the fundamental mode only. The higher mode properties, which contain the other dynamic properties of the superstructure, are of no interest for our purpose. Thus, for our study, a SDOF model is a simple and feasible model. The displacement time histories are ideal data for this purpose, the acceleration time histories are more likely to be contaminated by higher modes. A multiple degree of freedom model is required to accurately describe the complete acceleration time histories. However, because the frequencies of the higher modes are usually well separated from the fundamental mode, the high frequency signal contained in the accelerograms can be removed by using a low pass filter. Therefore, the filtered acceleration time histories are still useful for our purpose.

SECTION 3

ANALYTICAL SOLUTION FOR SDOF SYSTEM WITH A BILINEAR HYSTERETIC SPRING

3.1 General

An analytical solution for the quick-release nonlinear dynamic problem is desirable for checking the computer code used in the numerical method. The closed-form solution for the bilinear oscillator is also helpful to better understand the dynamic behavior of bilinear isolators. In the optimization problem, it also helps to reduce the time of computation. In this report, we provide an analytical solution for quick-release response of the SDOF system having a bilinear hysteretic spring. The typical hysteretic curve for the quick-release response of the bilinear model is shown in figure 3-1. The whole SDOF response for a bilinear model can be obtained by solving a sequence of linear problems. For simplicity, we assume that the total response curve is made up by three branches: elastic branch (segment 3-6), yielding branch (segment 6-8), and elastic tail (8-11). Unless the release displacement is very large, where five or more branches may be required to describe the whole response, the response of quick-release tests usually contain only these three branches. The general form of the equation of motion can be written as:

$$M\ddot{v}(t) + C\dot{v}(t) + K(t)v(t) = p(t) \quad (3-1)$$

$$K(t) = \begin{cases} K_i & (\text{branch 3-6 and 8-11.}) \\ K_d & (\text{branch 6-8}) \end{cases} \quad (3-2)$$

$$p(t) = \begin{cases} -F_y(-\alpha\beta + \alpha + \beta - 1) & (3-6) \\ F_y(1 - \beta) & (6-8) \\ (F_y + K_i v_8)(1 - \beta) & (8-11) \end{cases} \quad (3-3)$$

Here M , C , represent the mass and damping coefficient. $K(t)$ and $p(t)$ are stiffness and equivalent load. The value of $K(t)$ and $p(t)$ vary from branch to branch where F_y is the yielding force, α and β

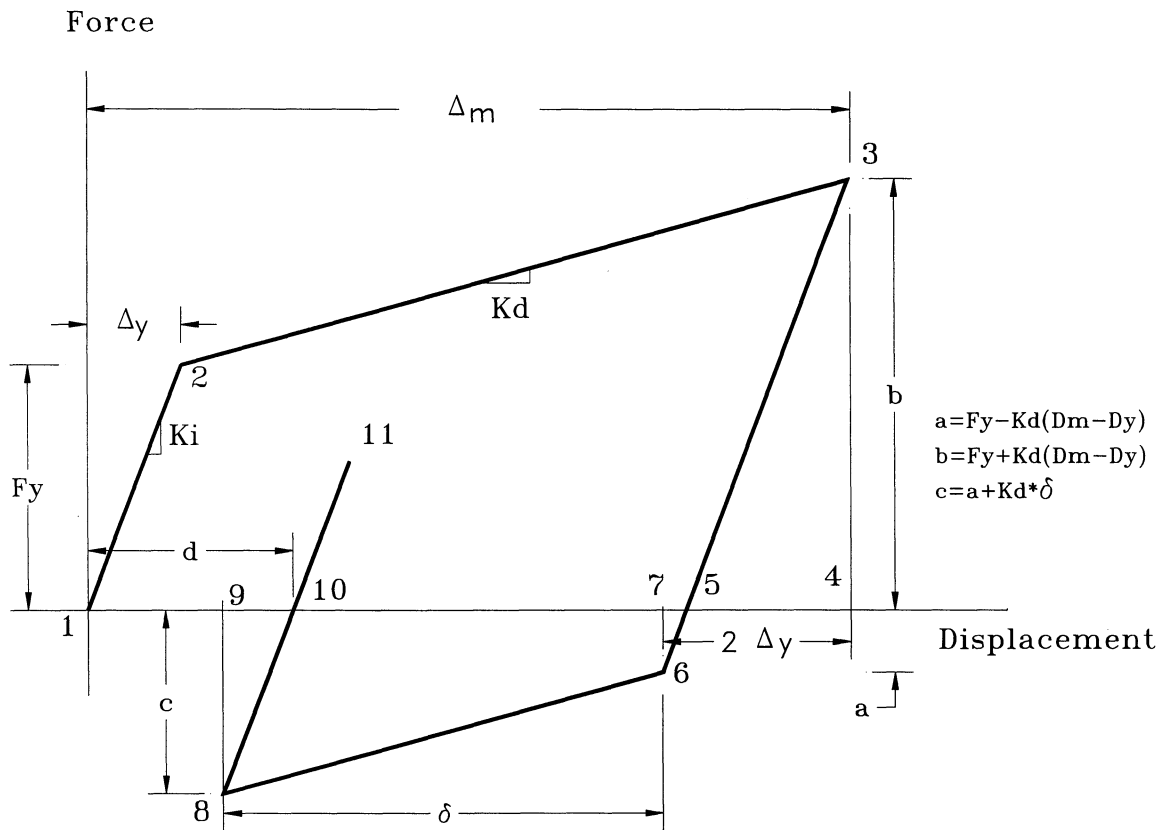


Figure 3-1 Definition of the Bilinear Model

are two dimensionless parameter defined by:

$$\alpha = \frac{\Delta_m}{\Delta_y} \quad (3-4)$$

$$\beta = \frac{K_d}{K_i} \quad (3-5)$$

In the equations above, Δ_m is the release displacement, and Δ_y the yield displacement. K_i and K_d are the initial and post yield stiffness respectively. The typical values of α for field tests may be between 2 and 20 and the range of values β for typical lead-rubber bearings may be between 0.015 and 0.35.

3.2 Analytical Solution for Zero Damping

When viscous damping is zero, the solutions for displacement and velocity time histories are:

$$v(t) = \begin{cases} \Delta_y[(1+\alpha\beta-\beta)\cos\omega t - (1+\alpha\beta-\beta-\alpha)] & (0 < t \leq t_6) \\ \Delta_y[-2\sqrt{\alpha-1}\sin\omega\sqrt{\beta}(t-t_6) + (\alpha - \frac{1}{\beta} - 1)\cos\omega\sqrt{\beta}(t-t_6) + \frac{1-\beta}{\beta}] & (t_6 < t \leq t_8) \\ d + (v_8 - d)\cos\omega(t-t_8) & (t > t_8) \end{cases} \quad (3-6)$$

$$\dot{v}(t) = \begin{cases} -\Delta_y\omega(1+\alpha\beta-\beta)\sin\omega t & (0 < t \leq t_6) \\ -\sqrt{\beta}\omega\Delta_y[2\sqrt{\alpha-1}\cos\omega\sqrt{\beta}(t-t_6) + (\alpha - \frac{1}{\beta} - 1)\sin\omega\sqrt{\beta}(t-t_6)] & (t_6 < t \leq t_8) \\ -\omega(v_8 - d)\sin\omega(t-t_8) & (t > t_8) \end{cases} \quad (3-7)$$

d is the permanent displacement:

$$d = \Delta_y \left(\frac{1}{\beta} - 1 \right) \left[1 - \sqrt{\beta^2 (\alpha^2 + 2\alpha - 3) + 2\beta(1 - \alpha) + 1} \right] \quad (3-8)$$

v_8 is the displacement at point 8 (See figure 3-1):

$$v_8 = \frac{\Delta_y}{\beta} \left\{ 1 - \beta - \sqrt{\beta^2 (\alpha^2 + 2\alpha - 3) + 2\beta(1 - \alpha) + 1} \right\} \quad (3-9)$$

t_6 and t_8 correspond to the times at which branch 6-8 and 8-11 are reached respectively. They are determined from:

$$t_6 = \frac{1}{\omega} \arccos \left[\frac{\beta(\alpha - 1) - 1}{\beta(\alpha - 1) + 1} \right] \quad (3-10)$$

$$t_8 = \begin{cases} t_6 + \frac{1}{\omega\sqrt{\beta}} \arctan \left[\frac{2\beta\sqrt{\alpha - 1}}{1 - \beta(\alpha - 1)} \right] & (\text{if } \alpha \leq \frac{1}{\beta} + 1) \\ t_6 + \frac{1}{\omega\sqrt{\beta}} \arctan \left[\frac{2\beta\sqrt{\alpha - 1}}{1 - \beta(\alpha - 1)} \right] + \frac{\pi}{\omega\sqrt{\beta}} & (\text{if } \alpha > \frac{1}{\beta} + 1) \end{cases} \quad (3-11)$$

For the zero damping case, equations (3-6) and (3-7) represent the quick-release response of the bilinear oscillator if the permanent displacement d is the positive. When α is large enough to cause a negative permanent displacement, more than three branches are required to represent the total response.

3.3 Analytical Solution for the Damped Case

The solution for the displacement and velocity response:

$$v(t) = \begin{cases} \Delta_y [\beta(\alpha-1)+1] e^{-\zeta\omega t} \left(\frac{\zeta\omega}{\omega_D} \sin\omega_D t + \cos\omega_D t \right) + \Delta_y (\alpha + \beta - \alpha\beta - 1) & (0 < t \leq t_6) \\ e^{-\zeta\omega(t-t_6)} \left[A \sin\omega_E(t-t_6) + B \cos\omega_E(t-t_6) \right] + \frac{\Delta_y(1-\beta)}{\beta} & (t_6 < t \leq t_8) \\ d + (v_8 - d) e^{-\zeta\omega(t-t_8)} \left[\frac{\zeta\omega}{\omega_D} \sin\omega_D(t-t_8) + \cos\omega_D(t-t_8) \right] & (t > t_8) \end{cases} \quad (3-12)$$

$$\dot{v}(t) = \begin{cases} -\Delta_y \frac{\omega^2}{\omega_D} [\beta(\alpha-1)+1] e^{\zeta\omega t} \sin\omega_D t & (0 \leq t \leq t_6) \\ e^{-\zeta\omega(t-t_6)} \{ A [-\zeta\omega \sin\omega_E(t-t_6) + \omega_E \cos\omega_E(t-t_6)] \\ - B [\omega_E \sin\omega_E(t-t_6) - \zeta\omega \cos\omega_E(t-t_6)] \} & (t_6 < t \leq t_8) \\ -(v_8 - d) \omega_D \left[\left(\frac{\zeta\omega}{\omega_D} \right)^2 + 1 \right] \sin\omega_D(t-t_8) & (t > t_8) \end{cases} \quad (3-13)$$

In equations (3-12) and (3-13), ζ is the damping ratio which is defined by:

$$\zeta = \frac{C}{2M\omega} \quad (3-14)$$

ω and ω_D are the elastic circular frequencies defined by:

$$\omega = \sqrt{\frac{K_i}{M}} \quad (3-15)$$

$$\omega_D = \omega \sqrt{1 - \zeta^2} \quad (3-16)$$

ω_E is the circular frequency corresponding to the yield branch:

$$\omega_E = \omega \sqrt{\beta - \zeta^2} \quad (3-17)$$

t_6 and t_8 are determined from:

$$e^{-\zeta\omega t_6} \left(\frac{\zeta}{\sqrt{1-\zeta^2}} \sin\omega_D t_6 + \cos\omega_D t_6 \right) = \frac{\beta(\alpha-1)-1}{\beta(\alpha-1)+1} \quad (3-18)$$

$$t_8 = \begin{cases} t_6 + \frac{1}{\omega_E} \arctan\left(\frac{\omega_E A - \zeta\omega B}{\zeta\omega A + \omega_E B}\right) & \left(\text{if } \frac{\omega_E A - \zeta\omega B}{\zeta\omega A + \omega_E B} \geq 0\right) \\ t_6 + \frac{1}{\omega_E} \arctan\left(\frac{\omega_E A - \zeta\omega B}{\zeta\omega A + \omega_E B}\right) + \frac{\pi}{\omega_E} & \left(\text{if } \frac{\omega_E A - \zeta\omega B}{\zeta\omega A + \omega_E B} < 0\right) \end{cases} \quad (3-19)$$

A and B are coefficients:

$$A = \frac{\Delta_y \zeta \omega}{\beta \omega_E} [\beta(\alpha-1)-1] - \frac{\Delta_y \omega^2}{\omega_E \omega_D} [\beta(\alpha-1)+1] e^{-\zeta\omega t_6} \sin\omega_D t_6 \quad (3-20)$$

$$B = \Delta_y \frac{1}{\beta} [\beta(\alpha-1)-1] \quad (3-21)$$

d is the permanent displacement:

$$d = (\Delta_y + v_8)(1 - \beta) \quad (3-22)$$

v_8 is the displacement at the point 8 which is determined from:

$$v_8 = e^{-\zeta\omega(t_8 - t_6)} [A \sin \omega_E(t_8 - t_6) + B \cos \omega_E(t_8 - t_6)] + \frac{\Delta_y(1 - \beta)}{\beta} \quad (3-23)$$

When conducting quick-release tests on lead-rubber bearings systems it is desirable to release the deformed system such that the final permanent displacement d is zero. We define α_0 to be that value of α which results in a zero permanent displacement. By equating the energy stored under the hysteretic loop in figure 3-1 defined by the points 3, 4 and 5 with the energy under the loop defined by points 5, 6, 8 and 9 a closed form solution for α_0 for the zero damped case can be derived:

$$\alpha_0 = \frac{2}{\beta} - 3 \quad (3-24)$$

For the damped case, we used a numerical method to find α_0 . Figure 3-2 shows the relations between α_0 and β . We can see that when $\beta < 0.1$, as β decreases, then α_0 increases rapidly. Thus α_0 is very sensitive to the damping ratio when $\beta < 0.1$.

There are three limiting cases for equations (3-12) and (3-13). The first case is when the response can not reach the second branch. This is possible when ζ is large and α is small. When α is smaller than the right hand side of (3-25), then the quick-release response is confined entirely on branch 3-6 in figure 3-1. This means that the viscous damping ratio is so large that the oscillator can not get to branch 6-8. The condition for which the response requires three or more branches is:

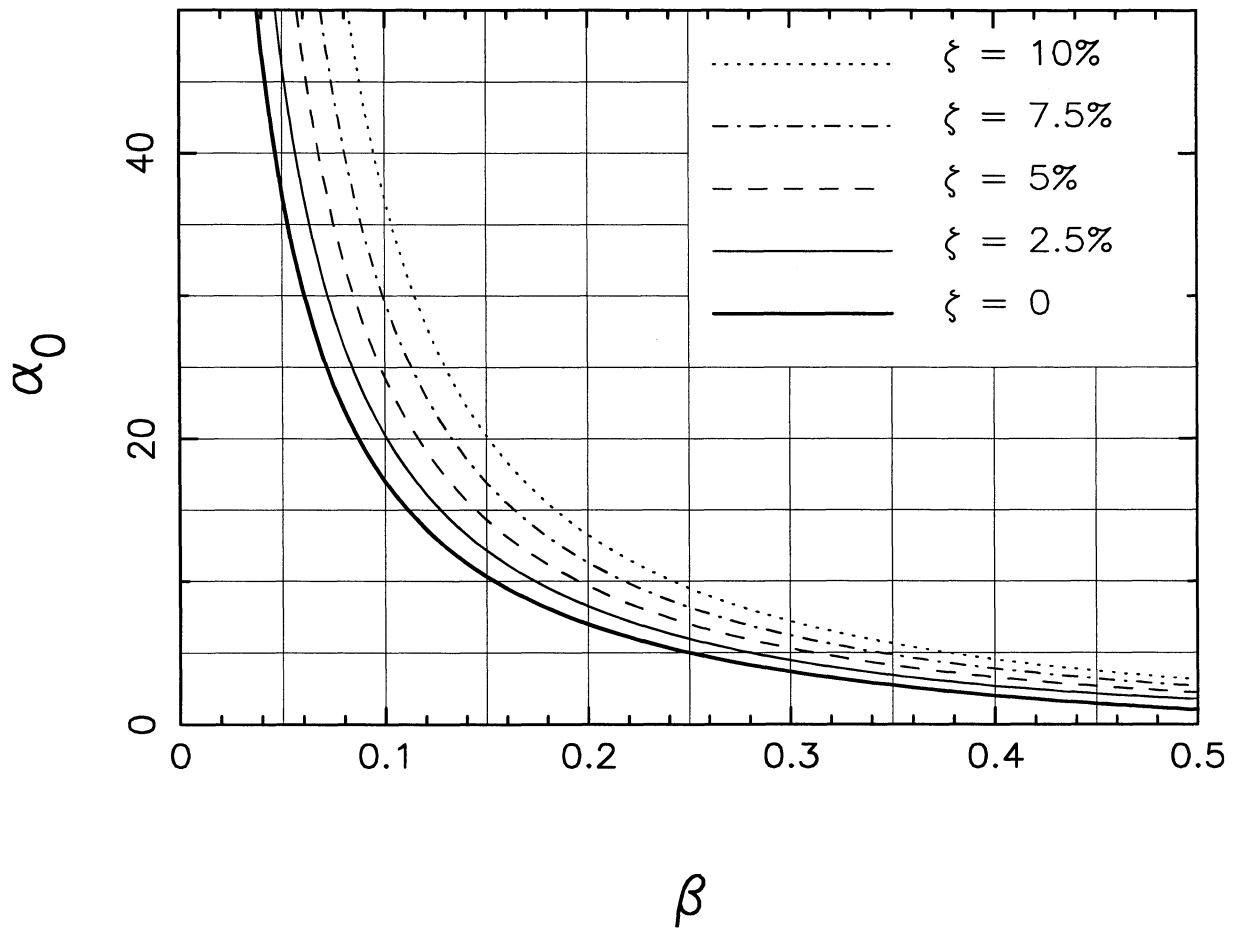


Figure 3-2 Relations between α_0 and β for Producing Zero Permanent Displacement

$$\alpha > \frac{1}{\beta} \left(\beta - 1 + \frac{2}{1 + e^{-\frac{\pi \zeta}{\sqrt{1-\zeta^2}}}} \right) \quad (3-25)$$

The second special case is when α is so large that more than three branches of the solution are required. In order to insure that no more than 3 branches (equations (3-12) and (3-13)) of the solution are required, v_g must satisfy equation (3-26):

$$v_g \geq - \left[1 + \frac{1}{\beta} \left(\frac{2}{1 + e^{-\frac{\pi \xi}{\sqrt{1-\xi^2}}}} - 1 \right) \right] \Delta_y \quad (3-26)$$

The third limiting case for solutions (3-12) and (3-13) is that the damping ratio ζ , which is defined by (3-14), should be smaller than the critical damping ratio of 1. For bilinear model, the critical damping is governed by the damping on yield branch (see (3-17)). For example, with a value of $\beta=0.1$, the critical damping ratio ζ would be about 30% on this branch of the hysteretic loop.

Finally it should be noted that the dynamic response of the bilinear hysteretic oscillator has a varying frequency due to the nonlinear nature of the problem. We define the nominal natural frequency of the system as the natural frequency (3-15) of the system during the elastic vibrations that take place on branch 8-11 in figure 3-1. From equation (3-15) it can be seen that in order to back calculate the initial stiffness K_i from the natural frequency, the mass M must be known. Thus, in order to apply this methodology, an accurate estimate of the dynamic mass must be made from the construction drawings.

SECTION 4

A GENERALIZED RAMBERG-OSGOOD MODEL AND ITS IMPLIED BILINEAR MODEL

4.1 Generalized Ramberg-Osgood Model

A generalized Ramberg-Osgood model proposed by Desai et al. (1976), which is found to be more flexible than the bilinear model, is utilized to simulate the hysteretic curves for the lead-rubber type isolators. The force-displacement relation of the Ramberg-Osgood model is described by:

$$\frac{F}{F_0} = \frac{\Delta}{\Delta_0} \left[\eta + \frac{1}{\left(1 + \left|\frac{\Delta}{\Delta_0}\right|^\gamma\right)^{\frac{1}{\gamma}}} \right] \quad (\text{Backbone}) \quad (4-1)$$

$$\frac{F-F_1}{F_0} = \frac{\Delta-\Delta_1}{\Delta_0} \left[\eta + \frac{1}{\left(1 + \left|\frac{\Delta-\Delta_1}{2\Delta_0}\right|^\gamma\right)^{\frac{1}{\gamma}}} \right] \quad (\text{Other Branches}) \quad (4-2)$$

where F and Δ are load and displacement respectively. F_1 and Δ_1 represent the coordinates of the most recent point on the hysteretic loop where the load changes direction (i.e. from increasing to decreasing). F_0 and Δ_0 are the characteristic yield load and characteristic yield displacement respectively. γ is an exponent parameter. η is a parameter which is related to the final stiffness. The Generalized Ramberg-Osgood model is defined by these four parameters, F_0 , Δ_0 , γ and η . The Generalized Ramberg-Osgood model becomes the standard Ramberg-Osgood model (Hibbeler, 1992) when η is equal zero. When η is greater than zero, and when γ is large, the model approximates the bilinear model very well. When η is equal to zero, and when γ is large, the model approximates the elasto-plastic model.

4.2 Implied Bilinear Model

Figure 4-1 shows curves of the Generalized Ramberg-Osgood model having different γ and the implied bilinear model. The implied bilinear model is defined as the backbone of the Ramberg-Osgood hysteretic loop obtained when γ approaches infinity. We see that when γ is large, the Generalized Ramberg-Osgood model is a very close approximation of the bilinear model. The initial stiffness K_i , post yielding stiffness K_d , yield displacement Δ_y and yield force F_y of the implied bilinear model are related to the parameters F_0 , Δ_0 and η as defined below:

$$\Delta_0 = \Delta_y \quad (4-3)$$

$$K_i = \frac{F_y}{\Delta_y} \quad (4-4)$$

$$F_0 = \frac{F_y}{(1+\eta)} \quad (4-5)$$

$$\eta = \frac{\beta}{1-\beta} \quad (4-6)$$

$$K_d = K_i \left(\frac{\eta}{1+\eta} \right) \quad (4-7)$$

Figure 4-2 shows the load-deformation relations for the generalized Ramberg-Osgood model and its implied bilinear model. Figure 4-3 shows the backbone branch of laboratory test data obtained at the

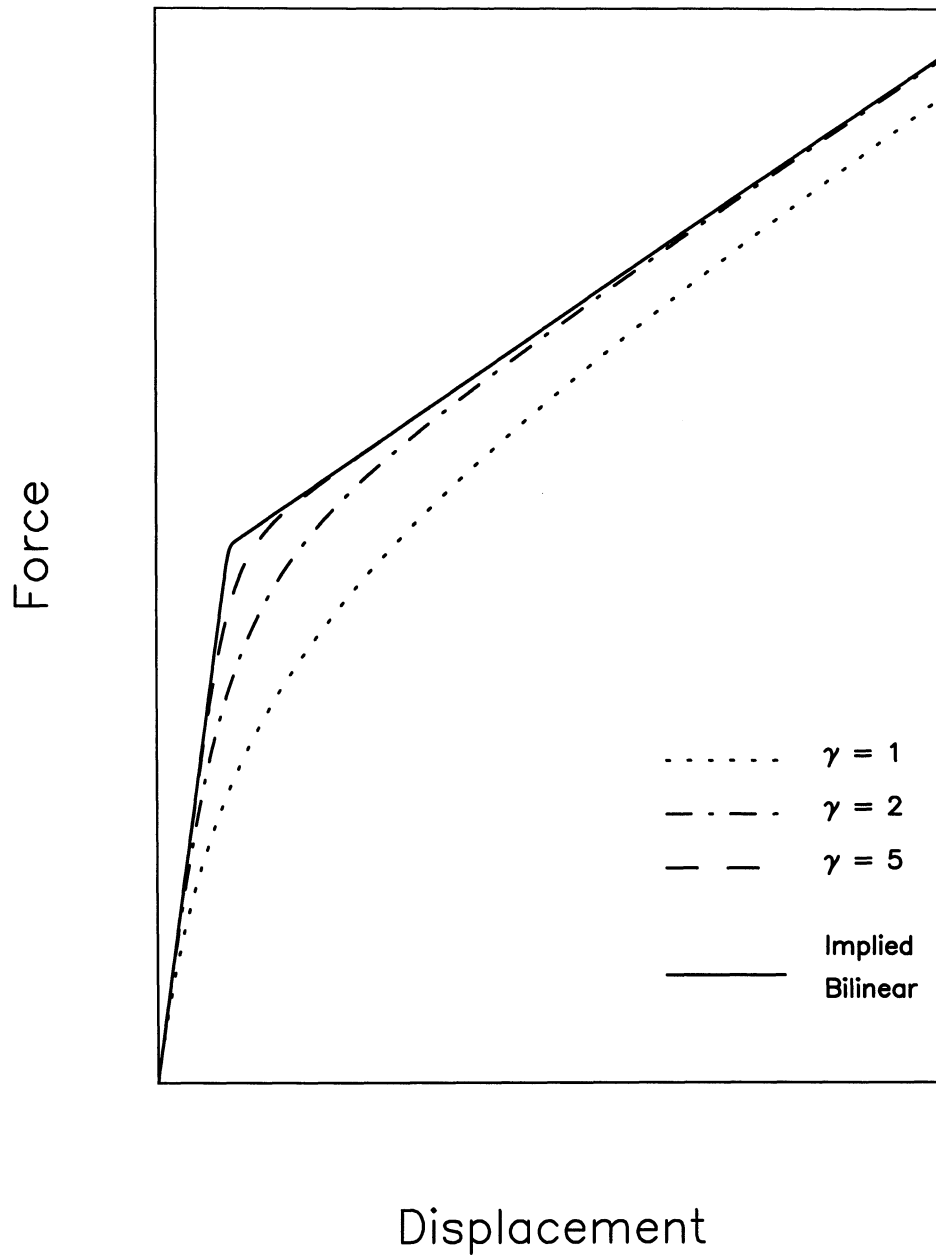


Figure 4-1 Generalized Ramberg-Osgood Model and Its Implied Bilinear Model

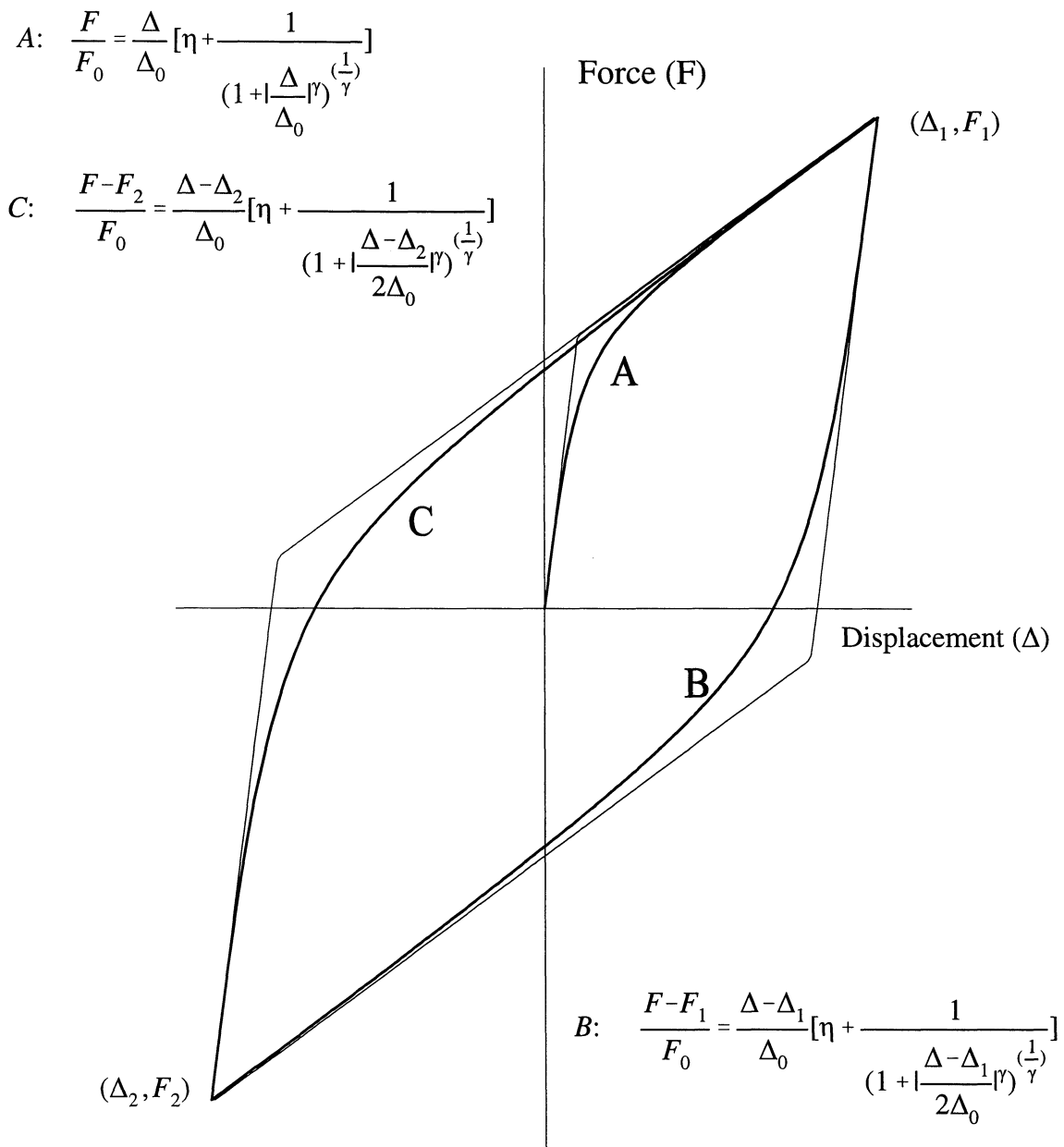
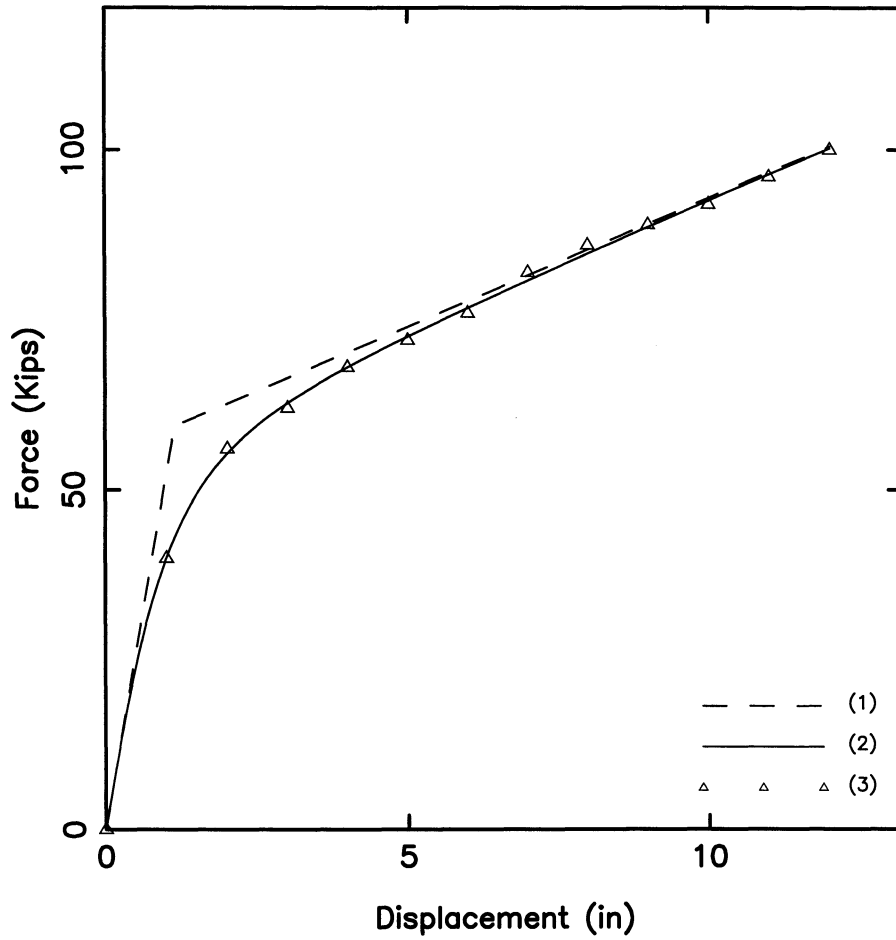


Figure 4-2 Definition of Generalized Ramberg-Osgood Model



- (1) Implied bilinear model.
- (2) Ramberg-Osgood fit to Force-Displacement data.
- (3) Experimental Force-Displacement data.

Figure 4-3 Comparison between the Hysteretic Model and Experimental Data

State University of New York at Buffalo (Wendichansky, 1996) for a lead-rubber isolator, and the generalized Ramberg-Osgood model obtained by fitting the data in the least squares sense. We can see that the generalized Ramberg-Osgood model fits the hysteretic curve of the lead-rubber isolator better than the bilinear model. Thus the generalized Ramberg-Osgood model is a more accurate model than the bilinear model for our purpose.

SECTION 5

IDENTIFICATION OF DYNAMIC PROPERTIES OF SEISMICALLY ISOLATED BRIDGES FROM THE QUICK-RELEASE TIME HISTORIES

5.1 Modeling for the Optimization Problem

The objective function for our problem is defined as follows:

$$\psi(\alpha, \beta, \gamma, \omega, \zeta) = w \frac{\sum_{i=1}^N [\ddot{v}(t_i)_{cal} - \ddot{v}(t_i)_{obs}]^2}{\sum_{i=1}^N \ddot{v}(t_i)_{obs}^2} + (1-w) \frac{\sum_{i=1}^N [v(t_i)_{cal} - v(t_i)_{obs}]^2}{\sum_{i=1}^N v(t_i)_{obs}^2} \quad (5-1)$$

where:

- $\ddot{v}(t_i)_{cal}$ = Calculated acceleration time history.
- $\ddot{v}(t_i)_{obs}$ = Observed acceleration time history.
- $v(t_i)_{cal}$ = Calculated displacement time history.
- $v(t_i)_{obs}$ = Observed displacement time history.
- N = Number of sample points.
- w = Weighting parameter between zero and one.

The values of the calculated acceleration and displacement time histories are a function of the model parameters $\alpha, \beta, \gamma, \omega, \zeta$. Our goal is to find a set of parameters $\alpha_j, \beta_j, \gamma_j, \omega_j, \zeta_j$ which make the objective function a global minimum:

$$\Psi_{min} = \Psi(\alpha_j, \beta_j, \gamma_j, \omega_j, \zeta_j) \quad (5-2)$$

The direct search algorithm proposed by Hooke and Jeeves (Hooke and Jeeves, 1961) was used to find the optimal parameters $\alpha_j, \beta_j, \gamma_j, \omega_j, \zeta_j$. The Hooke and Jeeves's search is started at some initial point $x_0 = x(\alpha_0, \beta_0, \gamma_0, \omega_0, \zeta_0)$. As is the case with most optimization problems, it is advantageous to choose the initial point in the space as close to the true solution as possible.

5.2 Numerical Procedure

A computer program was generated to solve for the parameters which minimize the objective function ψ . This program optimizes the parameters by comparing the calculated time histories with those which were obtained from full scale quick-release tests. The generalized Ramberg-Osgood and bilinear models are used for calculating the theoretical response, since the bilinear model is a special case for the Ramberg-Osgood model. Its solution was obtained by assigning a large number to the parameter γ in the generalized Ramberg-Osgood model. We assume that the mass of the SDOF can be independently determined and the initial displacement can be measured directly during the test. For the generalized Ramberg-Osgood model, there are five independent variables to be optimized. $(\alpha, \beta, \gamma, \omega, \zeta)$. For the bilinear model, there are only four variables $(\alpha, \beta, \omega, \zeta)$ because γ is fixed at a large number. Computational experience has shown that $\gamma = 20$ is large enough to simulate the bilinear model. The three parameters α, β, ω are connected to the five physical parameters $\Delta_m, \Delta_y, K_i, K_d, M$ through equations (3-4), (3-5) and (3-15).

The total damping effects of have been separated into two parts. The most significant damping in the system is caused by the hysteretic behavior of the isolators. The viscous damping, which causes the amplitude decay in the latter part of the time histories, has been defined by an independent parameter ζ . To determine all five physical parameters, we must know any two of them in advance. We assume the mass M and the initial displacement Δ_m can be determined independently. In the solution proposed here, we use both the observed accelerogram and the observed displacement time history to define the objective function in order to find the optimized solution.

The objective function we used is the summation of the displacement term and the acceleration term as shown in equation (5-1). Each term is defined by the sum of the square of differences between the calculated and observed time histories. In the case where the displacement time history is not available, we then substitute the displacement term with the square of differences between the calculated and observed permanent displacement weighted by the number of samples as mentioned above. We have found that the displacement term is necessary to fit the calculated permanent offset to the observed one. A step-by-step integration method (Clough and Penzien, 1976) is used to

calculate the theoretical time histories.

An example using the method is shown in figure 5-1. In this case we used a fictitious problem. First we generated a solution to a nonlinear SDOF system using the generalized Ramberg-Osgood hysteretic properties shown in the middle line of the table. In this case, the α , β and ω terms are derived from the implied backbone bilinear hysteretic curve in figure 4-3 associated with the Ramberg-Osgood model having a power term $\gamma = 2.5$ which was chosen for this example. We then used the optimization procedure to find the solution indicated in the third line of the table in figure 5-1. The initial values used to begin the optimization process are shown in line one of the table. The weighting factor w used in the objective function (4-1) was 0.5. The optimized solution is plotted as the solid line and the data to which it is being fit is the dashed line. The agreement between the calculated results and the “fictitious” data is excellent as can be seen in the top two subfigures. The Ramberg-Osgood force-displacement hysteretic curve that was found from the optimization process is shown in the lower subfigure of figure 5-1.

We also conducted a parameter study to see if the algorithm is robust for the range of parameters representing real isolation bearings. Clear limiting cases are represented by the $\beta = 1$ case which means that the system always remains elastic, and the other limiting case of $\beta = 0$. The $\beta = 0$ case represents the elasto-plastic case or the case of a bearing with infinite initial stiffness. For these cases, the algorithm we used breaks down. These are not serious limitations for the practical problem of real bridges isolated with lead-rubber bearings. For all cases we tried where $0.025 < \beta < 0.4$, $1.5 < \alpha < 40$ the algorithm is robust and solution can be found. A total of 400 cases were studied in this parameter investigation.

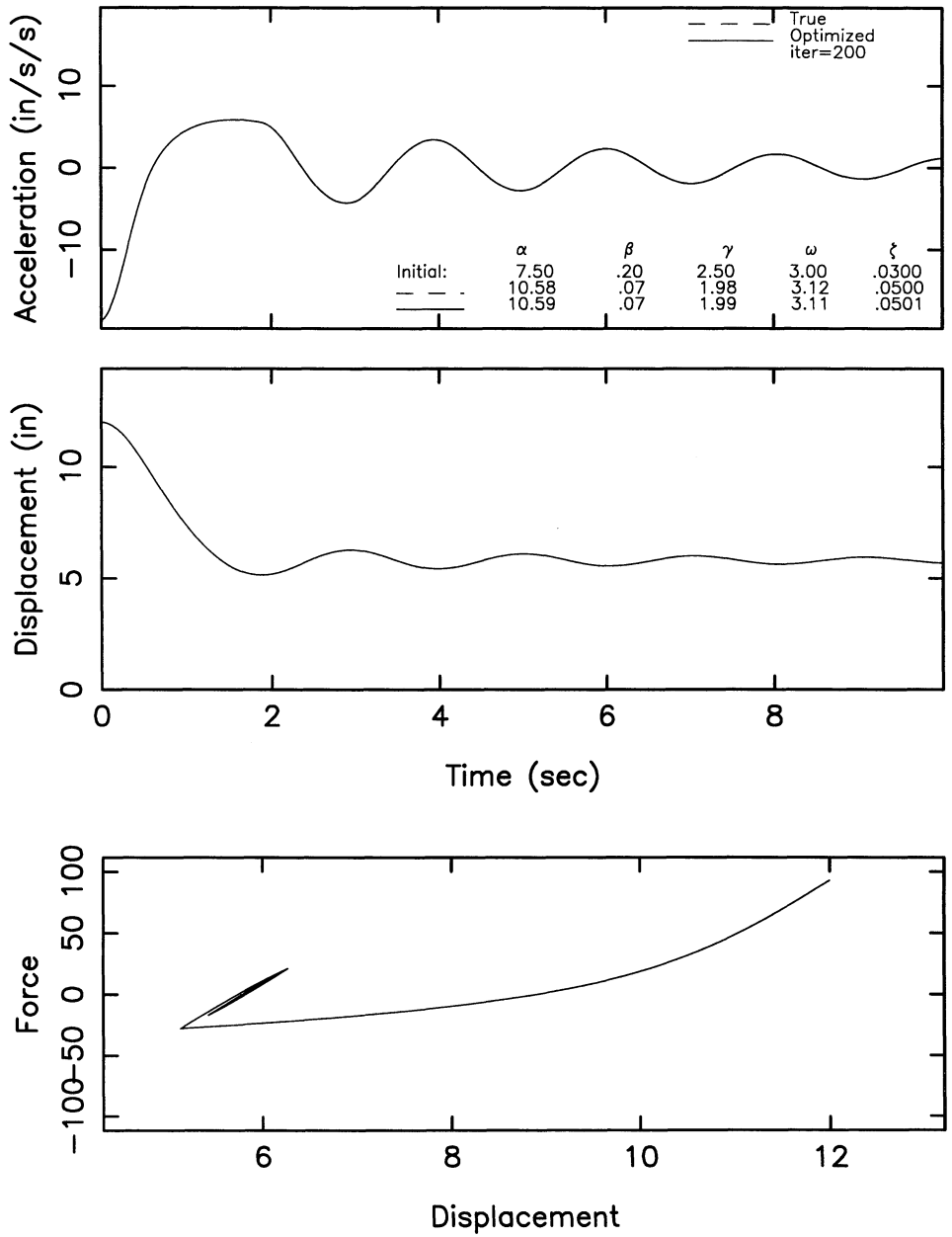


Figure 5-1 An Example for Parameter Identification

5.3 Parameter Identification Using Data from Full Scale Quick-Release Tests Conducted by University of California at Berkeley

In 1995 a full scale quick-release field tests for a seismically isolated bridge was carried out by the University of California at Berkeley. A detailed report was published by Gilani and others (Gilani et. al. 1995). The bridge tested is a four span seismically isolated viaduct in Walnut Creek, California. The deck system is isolated from the bents by 15 twenty-five cm (10 inch) high lead-rubber bearings.

A sequence of field tests including individual column quick-release tests, forced vibration tests and longitudinal quick-release tests of viaduct were conducted. Figure 5-2 shows the schematic of the viaduct deck. Figure 5-3 shows the acceleration and displacement time histories recorded on the viaduct during the quick release test which we used to estimate the hysteretic characteristics of the total isolation bearing system. The top curve is original acceleration time history which is dominated by a high frequency signal which is the longitudinal vibration mode of the superstructure (Gilani et. Al., 1995). A second order low-pass Butterworth filter was utilized to remove much of the high frequency contents. The phase shift caused by the filter processing was minimized by filtering the acceleration time history two times, once in the forward direction once in the backward direction. The middle curve in figure 5-3 shows the filtered acceleration time history. Comparing to the top curve in figure 5-3 we can see that the high frequency signal can be removed significantly by the low pass filter. The bottom curve in figure 5-3 is the displacement time history recorded during the test.

Figure 5-4 shows the optimization result using the generalized Ramberg-Osgood model, and figure 5-5 shows the optimization result using the bilinear model. By comparing the parameters obtained by both models in figures 5-4 and 5-5 we see that the bilinear and the generalized Ramberg-Osgood model give similar results. In figure 5-6, the triangle symbols show the experimental load deflection curve measured by Gilani et al. (1995) during the loading sequence for their structure. The dashed lines show the bilinear load deflection that Gilani et al. (1995) estimated from laboratory tests they conducted on the isolation bearings prior to their installation in the bridge. This curve was obtained by summing the load deflection curves of all the bearings installed in the bridge, and thus represents the total stiffness of the isolation system. The solid line bilinear force deflection relation shown in the

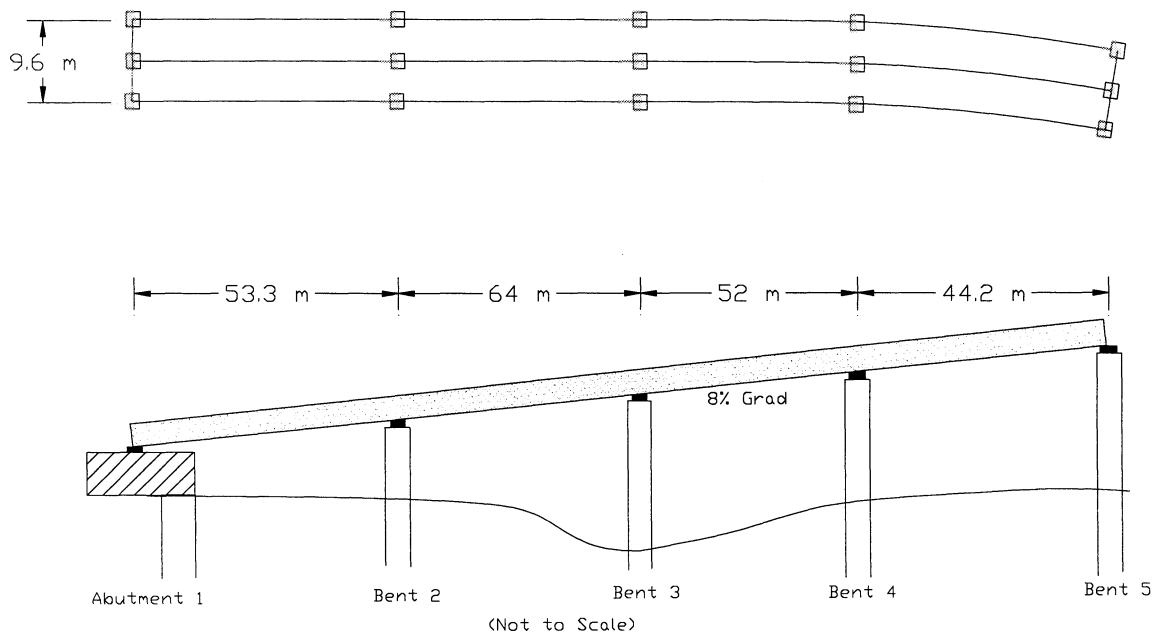


Figure 5-2 A Sketch of the Seismically Isolated Viaduct in Walnut Creek, California

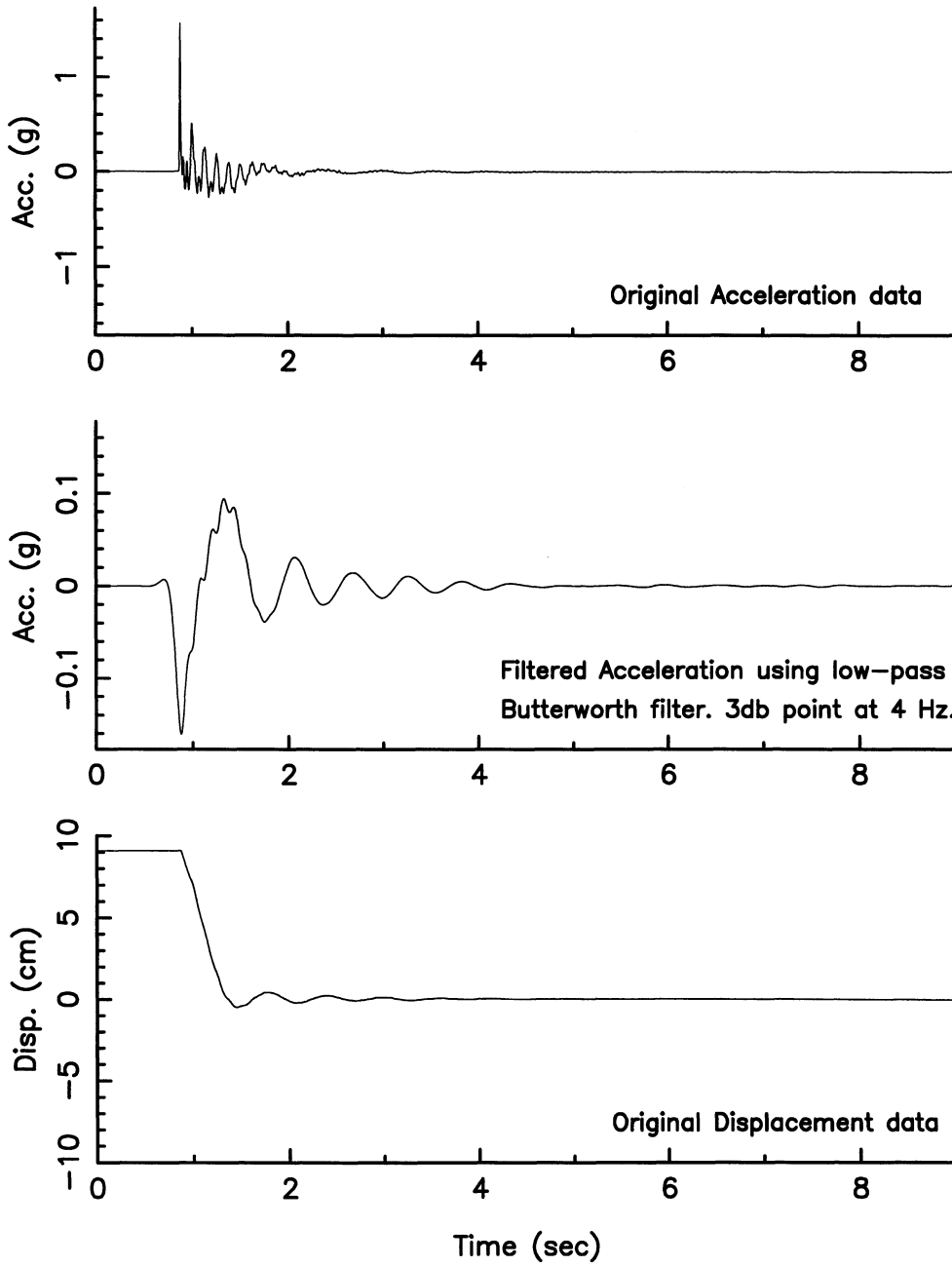


Figure 5-3 Time Histories for the Quick-Release Test Conducted by University of California at Berkeley

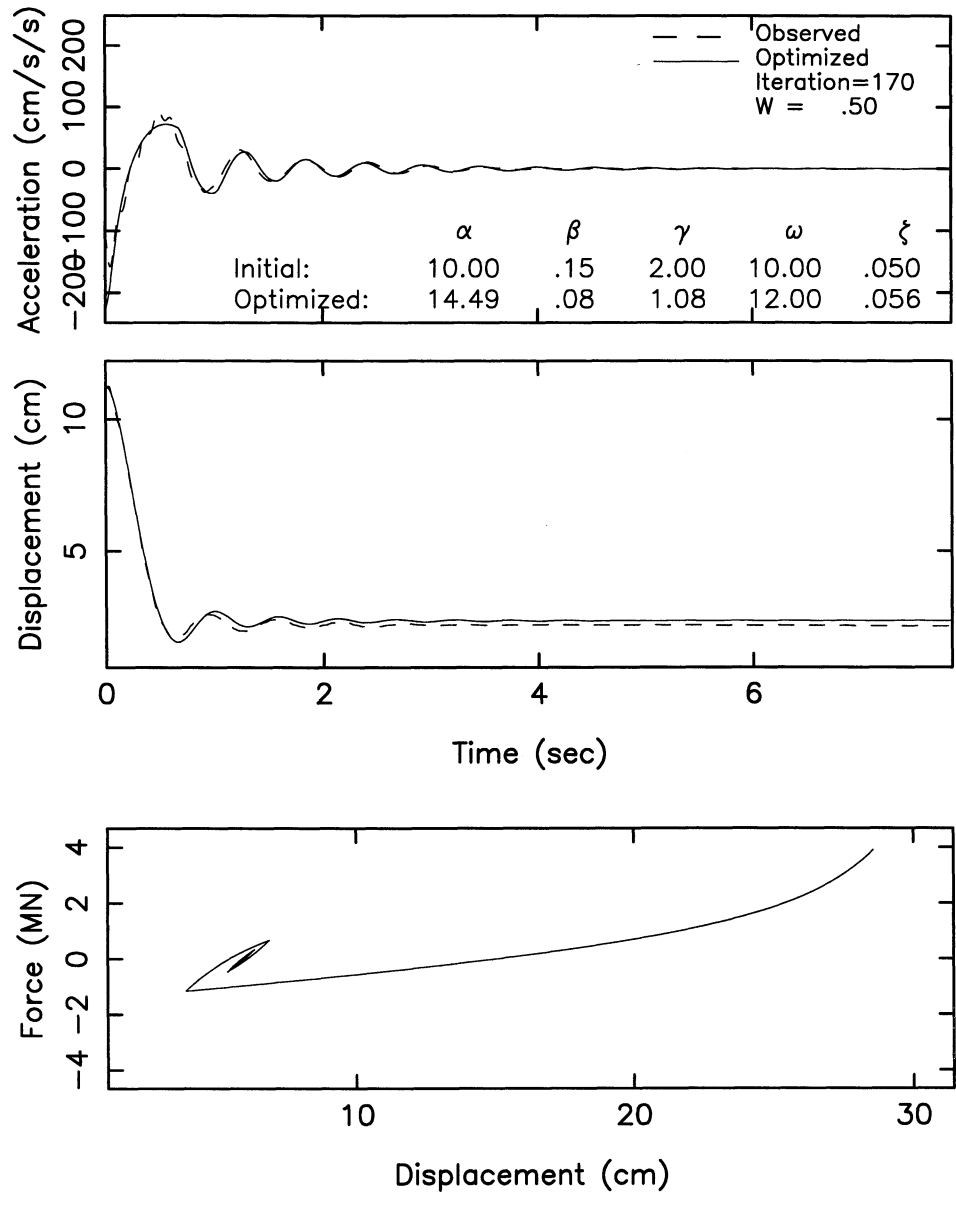


Figure 5-4 Optimization Results Using Generalized Ramberg-Osgood Model and the Quick-Release Testing Data from UC Berkeley

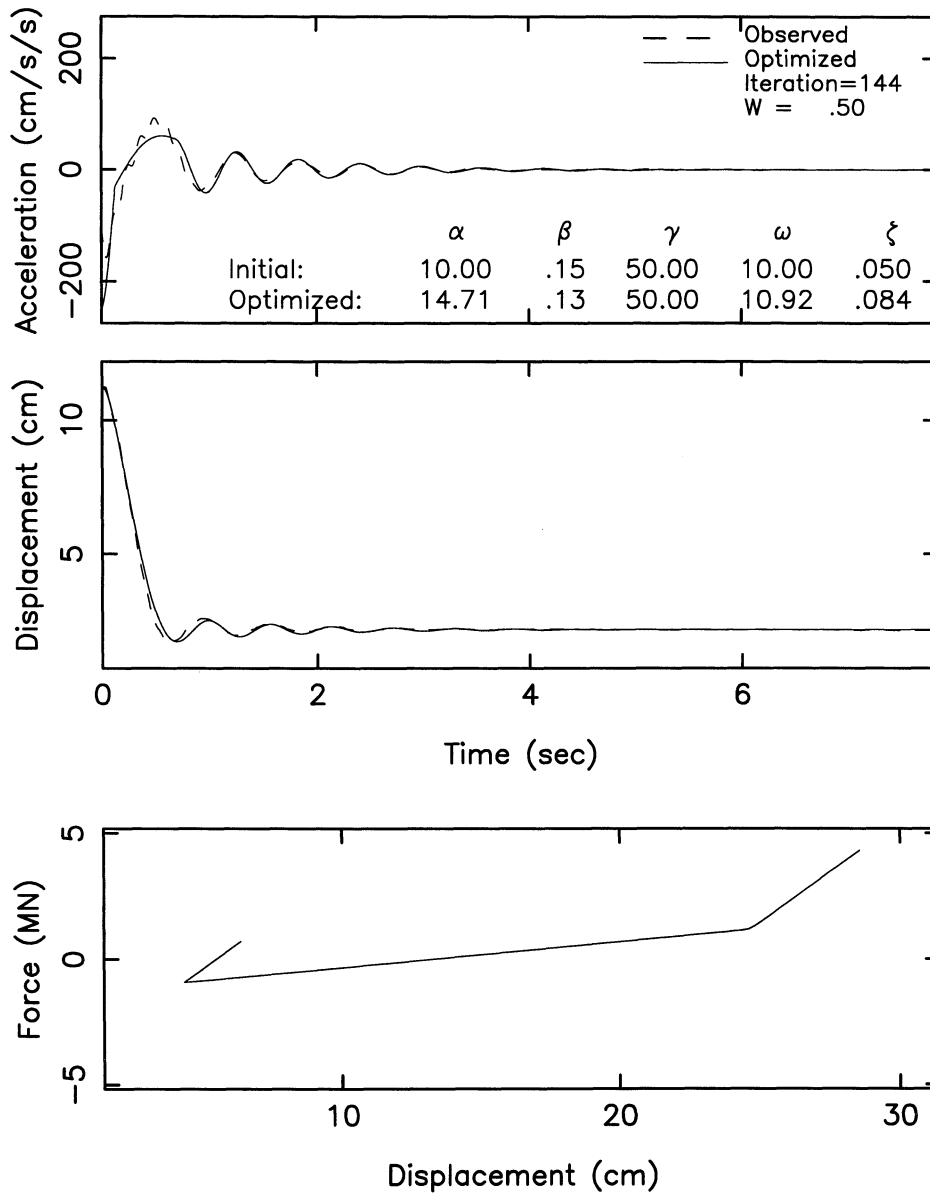


Figure 5-5 Optimization Results Using Bilinear Model and the Quick-Release Testing Data from UC Berkeley

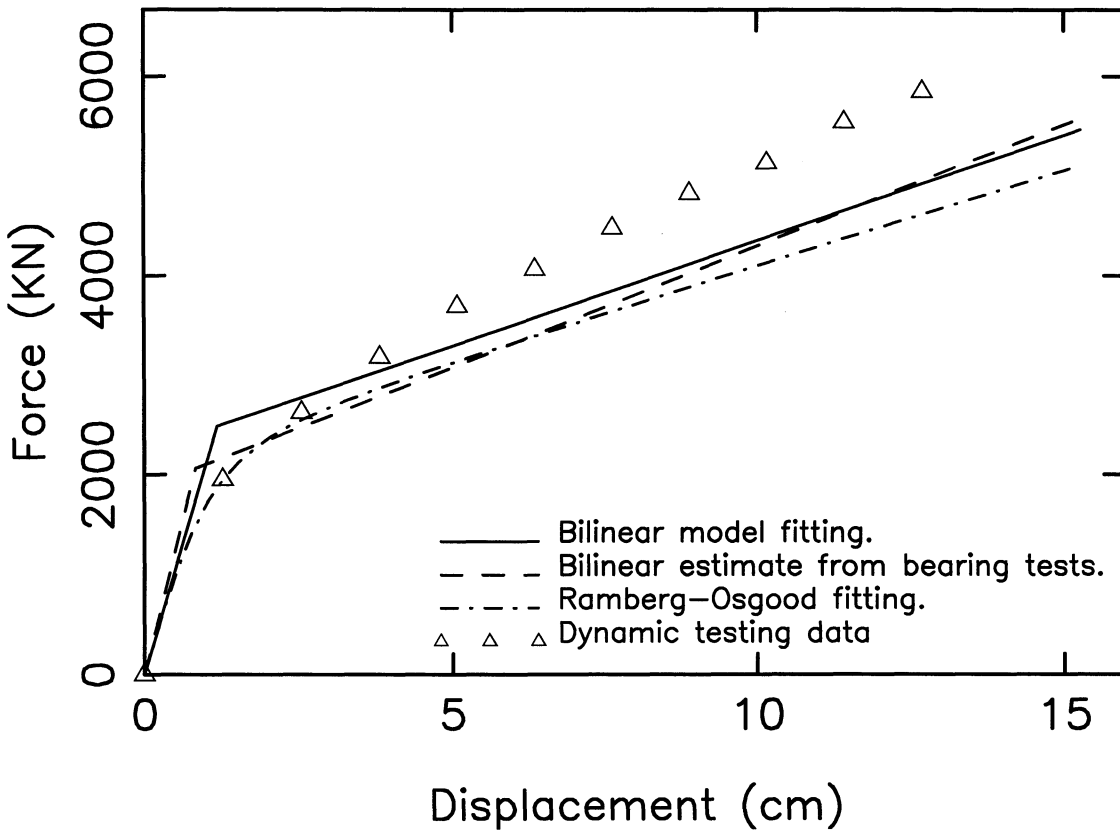


Figure 5-6 Force - Displacement Curves for Bearing Tests and Optimization Results

figure represents the result we obtained by using the bilinear hysteretic model in our optimization calculations. This was generated from the solution shown in figure 5-5. Finally, the dot dashed curve represents the backbone generalized Ramberg-Osgood curve we generated from the optimization procedure, which was obtained from the results shown in figure 5-4.

The range of the viscous damping ratio we estimate for this problem is 5.6% to 8.4% depending upon whether we use the Ramberg-Osgood model or the bilinear hysteretic model. Gilani and others (1995) determined that viscous damping ratio was 7% in good agreement with our result. We find that the natural frequency of the system in the elastic regime to be between 1.74 Hz and 1.97 Hz as determined by the bilinear and Ramberg-Osgood models respectively. It should be noted that the estimate of natural frequencies obtained from the bilinear model is probably more accurate than that from the Ramberg-Osgood Model. This is so because the Ramberg-Osgood natural frequency is that computed from the initial slope of the force deflection curve, while the bilinear model generate an “average” straight line initial slope from which the natural frequency is calculated. If one computes the natural frequency in the “elastic tail” of the Ramberg-osgood computation one finds that the natural frequency is 1.8 Hz which is smaller than the 1.91 Hz estimated from the initial stage. And it is in better agreement with the 1.74 Hz estimated from the bilinear model.

TABLE 5-1 Summary of the Optimization Results Using UC Berkeley’s Quick-Release Data

Models	Total Mass (Ton)	Final Disp. (cm)	Ductility Ratio (α)	Stiffness Ratio (β)	Power Factor (γ)	Elastic Frequency ($\omega/2\pi$, Hz)	Viscous Damping (ζ)
Bilinear	1723.6	2.14	14.71	0.13	50 (fixed)	1.74	8.4%
Ramberg-Osgood	1723.6	2.14	14.49	0.08	1.08	1.91	5.6%

Finally, it should be noted that our results underestimate the experimental field result for the force deflection curve in figure 5-6. It is our opinion that this is due to the fact that the hydraulic jack

pressure dropped from 50 MPa to 35 MPa during the 30-40 minutes proceeding the time when the structure was quick-released. This allowed the strain energy stored in the bearings to decay just prior to the quick-release. The optimization results for both bilinear model and Ramberg-Osgood model are summarized in Table 5-1.

5.4 Parameter Identification Using Data from State University of New York at Buffalo

Another quick-release field test was carried out in 1994 at the National Center for Earthquake Engineering at the State University of New York at Buffalo. A detailed description for this test is given by Wendichansky (1995, 1996). The tests were carried out on a pair of seismically isolated highway bridges (one southbound and one northbound) over Cazenovia Creek in New York State. Both bridges are typical three span slab on girder bridges with a small skew angle of about 10 degrees. A series of different tests were conducted on the bridges. As an example, we selected the time histories recorded from a quick-release test on southbound bridge in the transverse direction. Figure 5-7 shows the bridge elevation and section and the instrumentation locations for the data used in our optimization. Figures 5-8 through 5-9 show the displacement and acceleration time histories measured at the piers at the points shown in figure 5-7. These records contain a small amount of twisting of the deck. We reduced the effect of the twisting component by averaging the time histories measured on the north and south piers. Figure 5-10 shows the averaged acceleration and displacement time histories respectively. Strictly speaking, the superposition method is not valid for a nonlinear problem, but we used the averaging process because the twisting component is small compared to the transverse motion.

Two different types of bearings were installed on the bridge. Rubber bearings having low energy dissipation characteristics were installed over the two piers while high damping lead-rubber bearings were installed at the abutments. By using the technique presented in herein, only the hysteretic properties of the total isolation system consisting of all the bearings can be obtained. Figure 5-11 shows the optimization results using the generalized Ramberg-Osgood model. Figure 5-12 shows the optimization results using bilinear model. In both cases we used the averaged acceleration and the

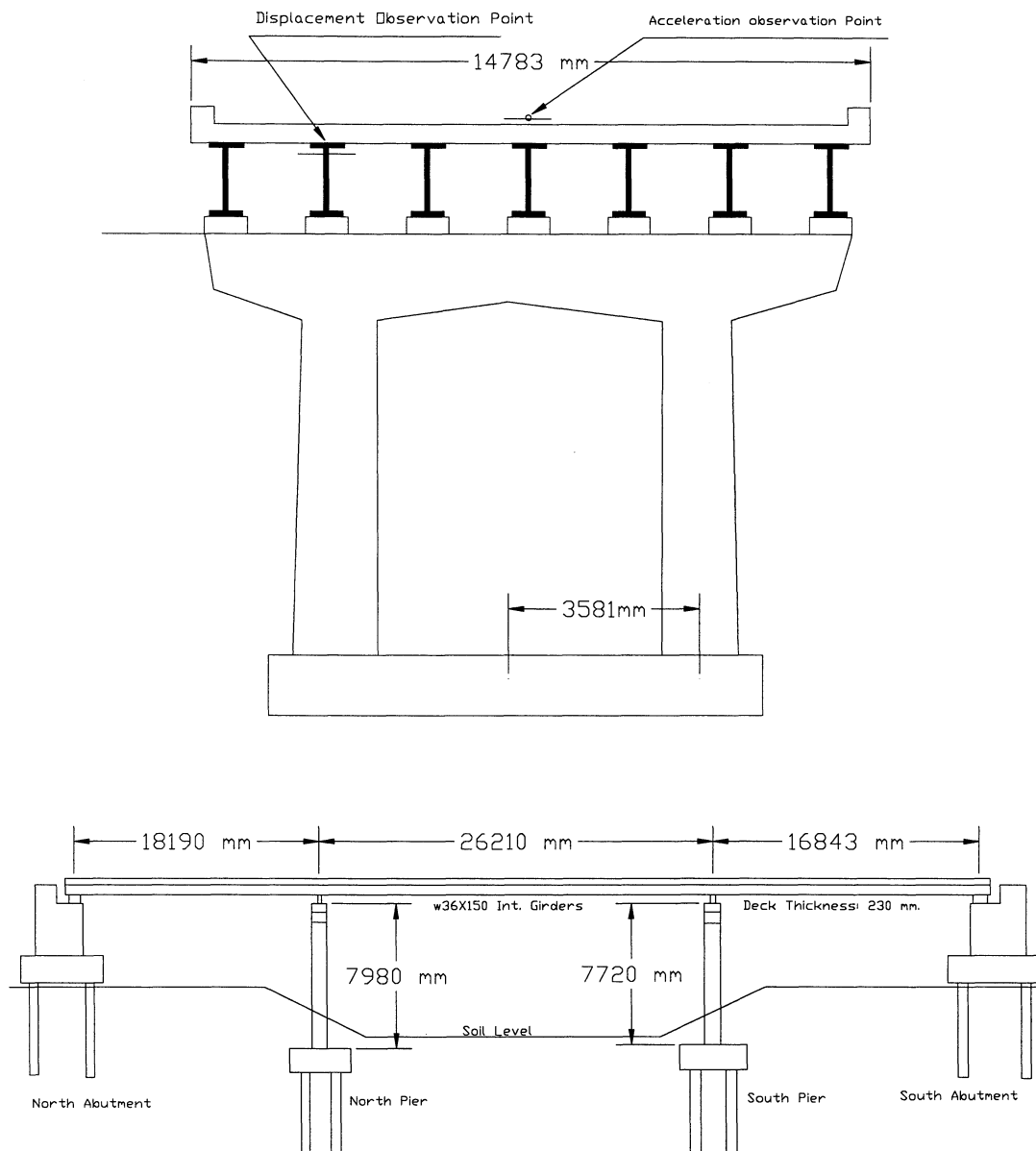


Figure 5-7 Plan and Side Views of Cazenovia Creek Bridge in New York State

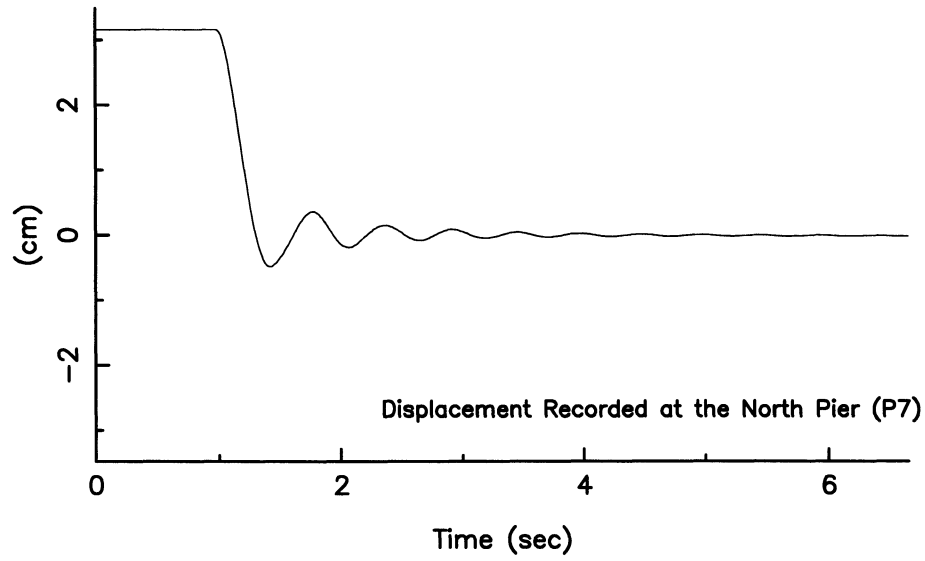
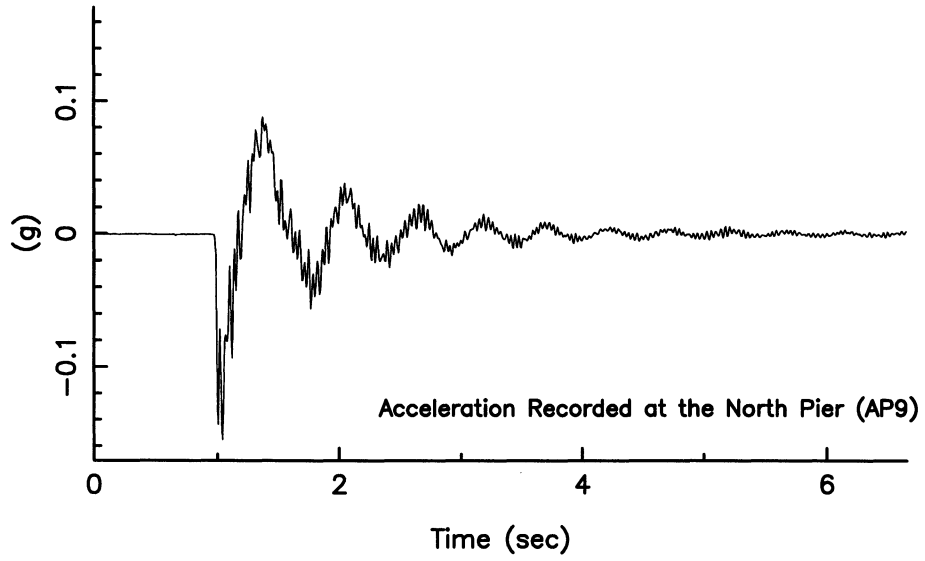


Figure 5-8 Acceleration and Displacement Time Histories Measured at the North Pier

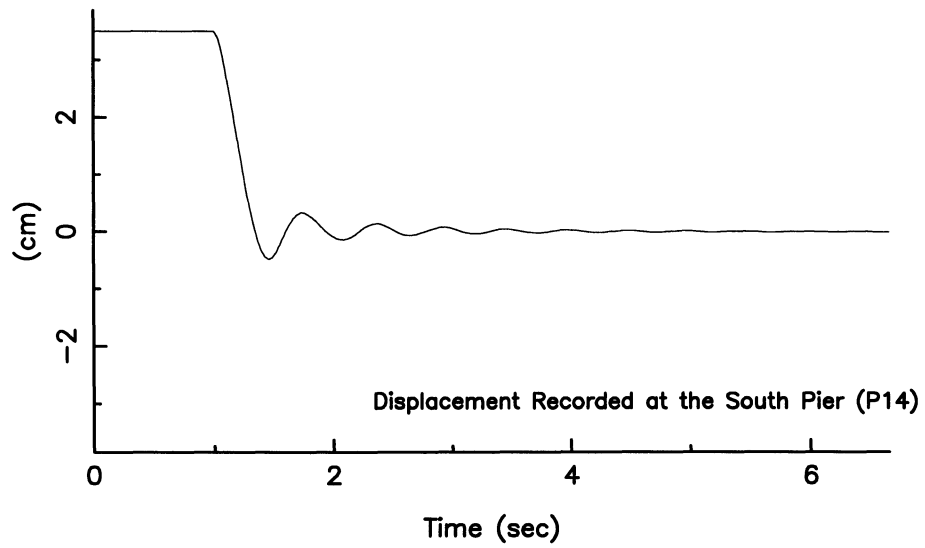
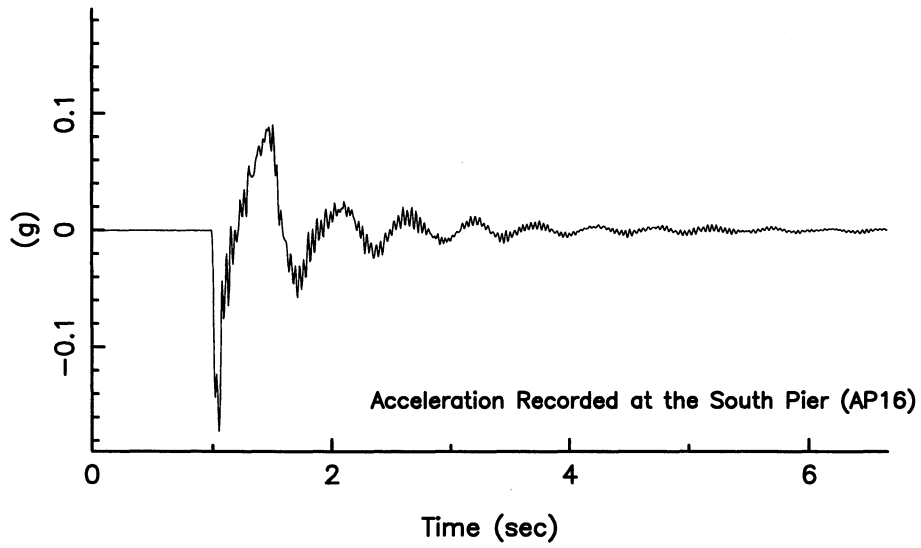


Figure 5-9 Acceleration and Displacement Time Histories Measured at the South Pier

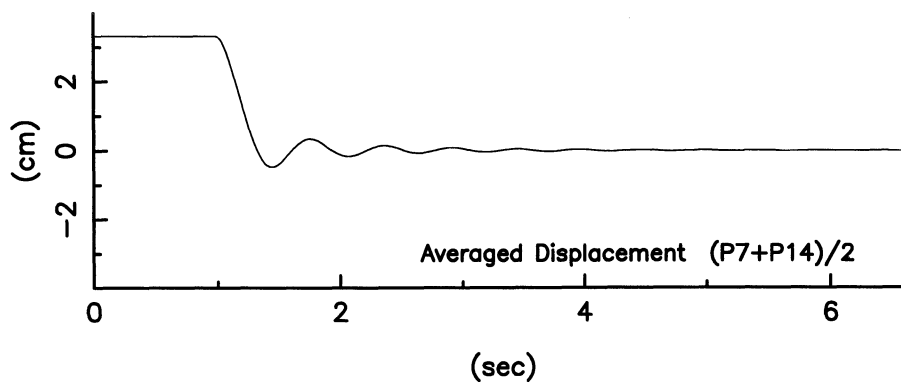
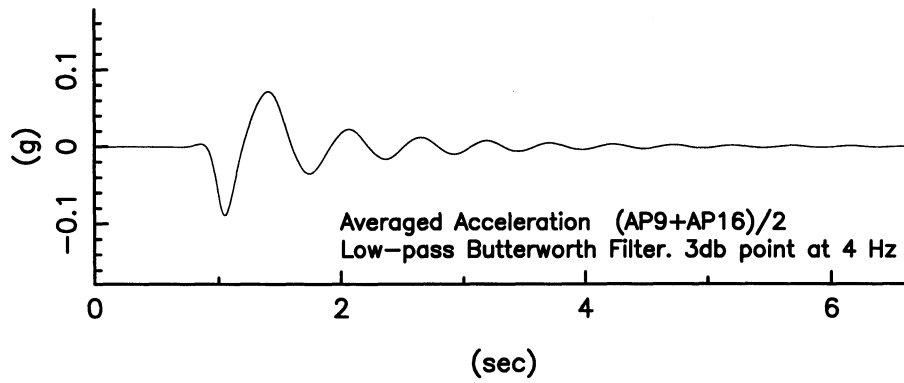
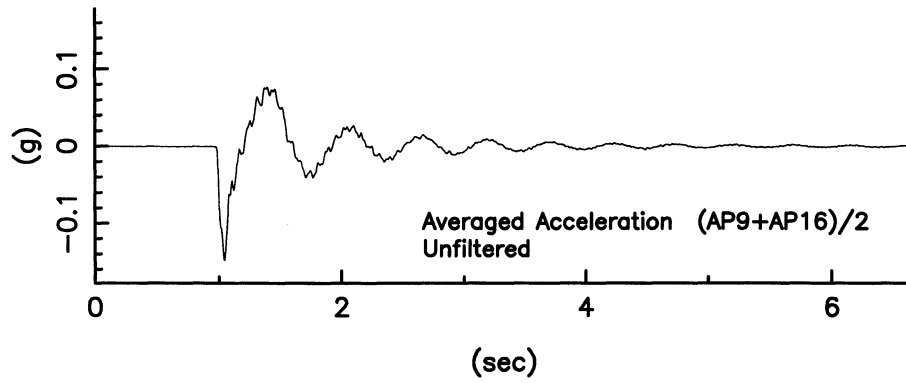


Figure 5-10 Averaged Time Histories for the North and South Piers

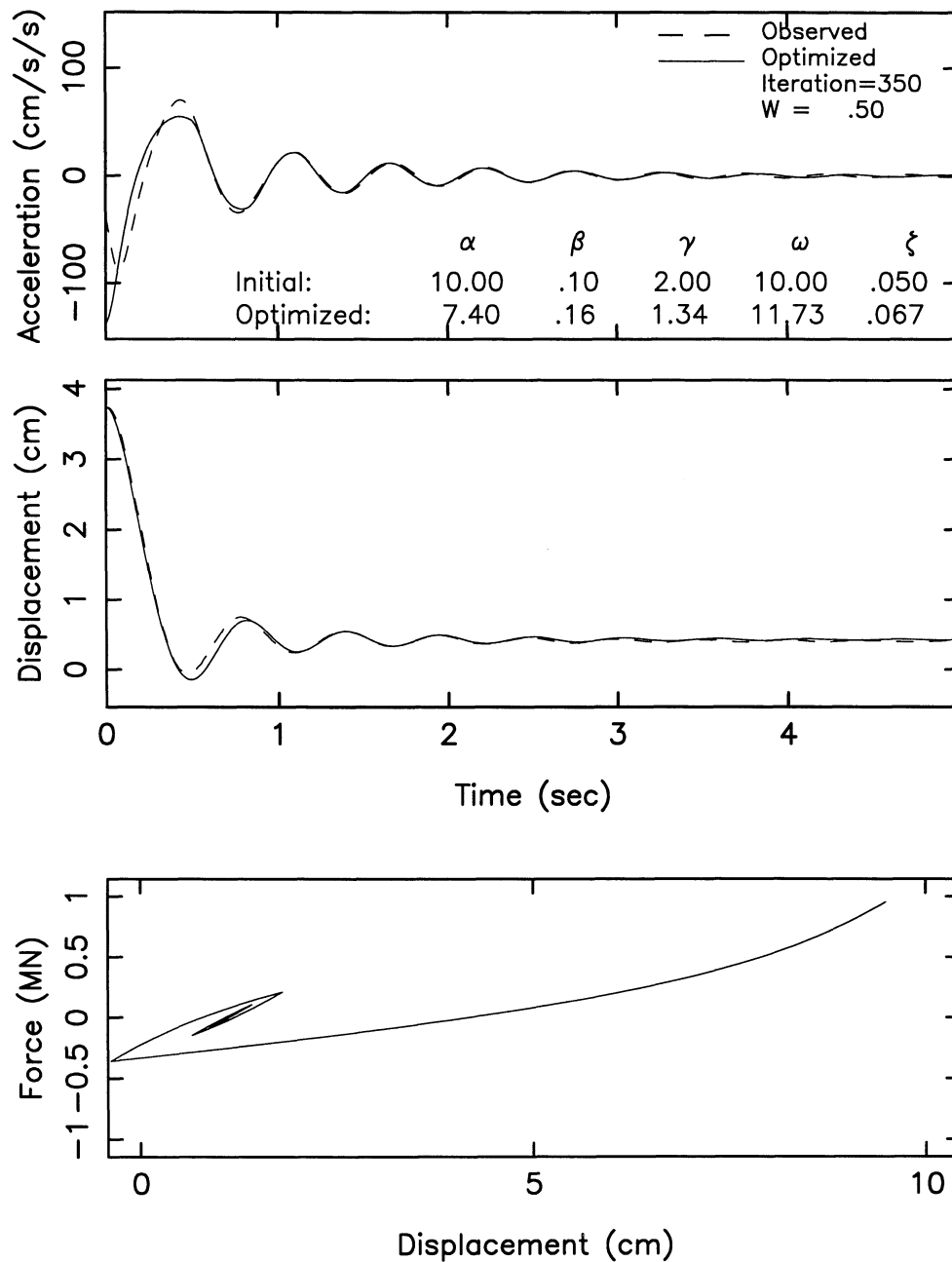


Figure 5-11 Optimization Results Using the Generalized Ramberg-Osgood Model and the Quick-Release Testing Data from State University of New York at Buffalo

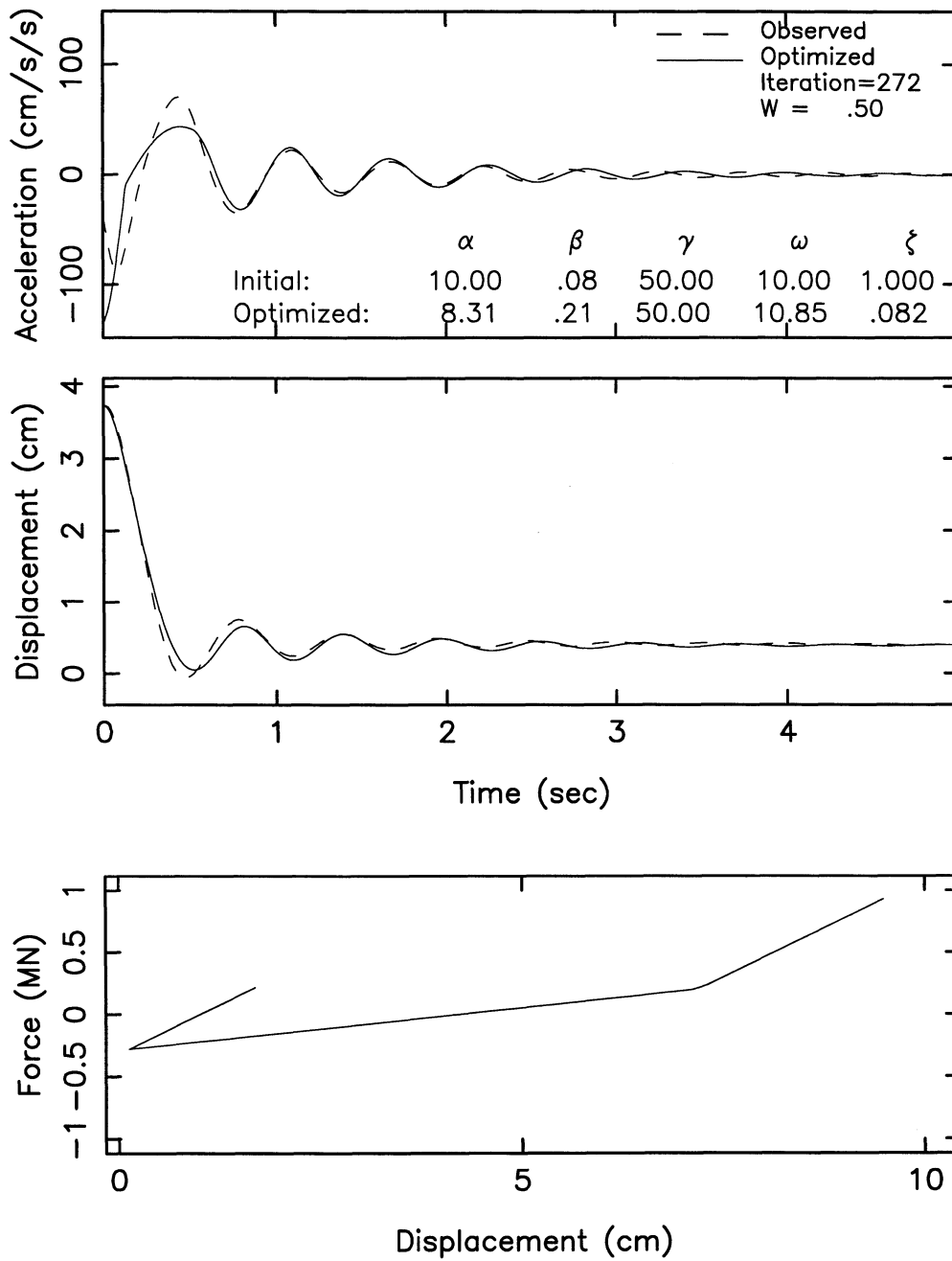


Figure 5-12 Optimization Results Using Bilinear Model and the Quick-Release Testing Data from State University of New York at Buffalo

displacement time histories as showing in figure 5-10. The averaged acceleration time history used in both case was filtered two times, once in the forward direction and once in the reverse direction using a second order low pass Butterworth Filter. The weighting factor w in the objective function (4-1) was taken to be 0.5 for both cases. Due to the twisting motion and the flexural deformation of the superstructure, the acceleration time history does not represent a single degree of freedom response at the beginning of the record. The twisting component of the superstructure can be seen by calculating the difference of the acceleration and displacement time histories measured at the north and south piers. It was found that the twisting motion is concentrated in the first one second of the signal and dies down rapidly thereafter. In the first second of the displacement record, the amplitudes of the twisting component of is about two percent of the amplitude of the transverse component. In this same initial time interval, the amplitudes of twisting component of the acceleration time history is about 25 percent of the transverse component. Therefore the first 1 second of accelerogram was ignored during the calculation of objective function (4-1) to remove the contamination by the twisting component. In figures 5-11 and 5-12 the optimized solution can be seen to fit the displacement and acceleration time history quite well except at the initial part of the acceleration record.

In the table in figure 5-11 the numerical values of the generalized Ramberg-Osgood model which were obtain are listed. The initial release displacement was 7.4 times the nominal yield displacement of the implied bilinear model associated with the Ramberg-Osgood model. The stiffness K_d was found to be 16% of K_i and the natural frequency of the elastic vibrations was 1.86 Hz. This compares reasonably with (1.96 Hz) found by Wendichansky (1996) using the Fourier spectrum of the elastic portion of the acceleration time histories. The viscous damping ratio we found were 8.2% for bilinear model and 6.7% for Ramberg-Osgood model. Using the logarithm decrement method. Wendichansky (1996) found the average value of the damping ratio for the third and fourth cycles of the displacement time histories at the north and south abutment to be 8%, which compares well with our result for the bilinear model. The optimization results are summarized in Table 5-2.

In Table 5-2, the total mass was estimated by calculating the weight of steel girders and deck. The permanent displacement was obtained by averaging the residual displacements recorded at the north

and south piers which was given by Wendichansky (Table 2-IX, Wendichansky, 1996). We have found that the permanent displacement is a very important value for our optimization method. The power factor for bilinear model was fixed at 50.

**TABLE 5-2 Summary of the Optimization Results
Using NCEER Quick-Release Testing Data**

Models	Total Mass (Ton)	Final Disp. (cm)	Ductility Ratio (α)	Stiffness Ratio (β)	Power Factor (γ)	Elastic Frequency ($\omega/2\pi$, Hz)	Viscous Damping (ζ)
Bilinear	689	0.406	8.31	0.21	50 (fixed)	1.72	8.2%
Ramberg-Osgood	689	0.406	7.4	0.16	1.34	1.86	6.7%

The bottom subfigure of figure 5-11 shows the load- displacement curve for the generalized Ramberg-Osgood model defined by the parameters given in the table in the figure 5-11. Figure 5-13 shows the total force displacement relationship constructed from laboratory test data (Wendichansky, 1996) obtained for the individual bearings prior to their installation in the bridge. To construct the curve represented by the solid line in the figure we summed the hysteretic loops obtained from these laboratory tests for both types of bearings which were installed in the bridge to generate the composite hysteretic loop shown in figure 5-13. We then generated the dashed line hysteretic loop from the model we obtained in figure 5-11 using the actual field test data. The agreement between the two is good.

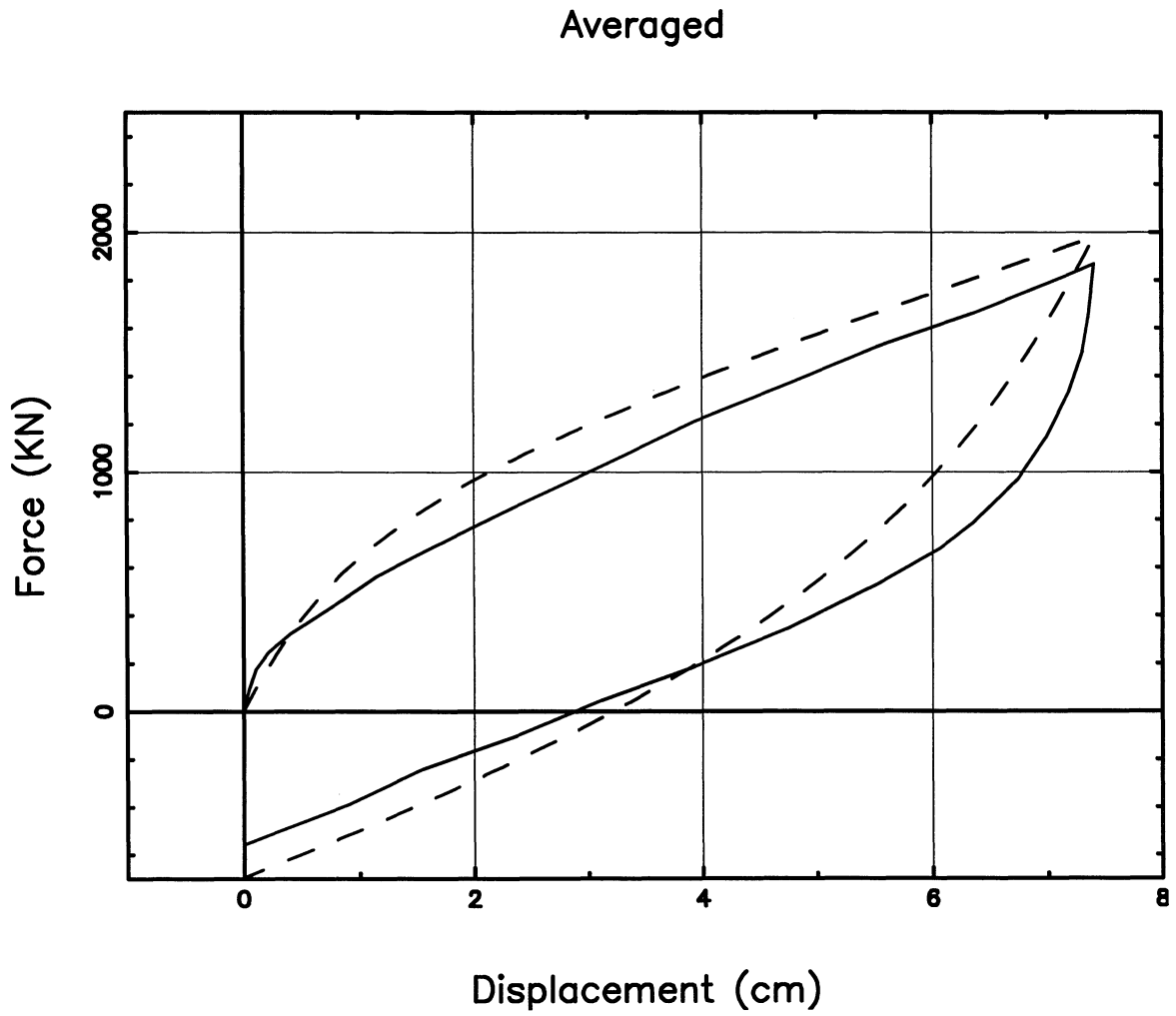


Figure 5-13 Comparison the Hysteretic Loops Between the Optimization Results and Laboratory Tests

SECTION 6

CONCLUSIONS

Based upon the two examples presented in this report, we have shown that quick-release field test data can be used to accurately extract the nonlinear hysteretic properties of seismically isolated bridges by using nonlinear SDOF models. Quick-release field test data was successfully used in conjunction with an optimization algorithm discussed in the report to identify the in-situ hysteretic properties of the isolated bridge system as well as the viscous damping coefficient and the fundamental frequency of the system during the elastic part of the response regime.

In order to implement the method, the dynamic mass of the system must be obtained by independent means from the construction drawings and field observations. In addition, both the acceleration and displacement time history responses must be measured. The high frequency content of the accelerogram contributed by the higher modes can be filtered out using a lowpass filter.

The generalized Ramberg-Osgood hysteretic rule was found to be an effective efficient nonlinear constitutive relationship for the purpose of investigating the SDOF behavior of bridges isolated with combinations of rubber and lead-rubber bearings. It is convenient because either the generalized Ramberg-Osgood rule or the bilinear hysteretic rule can be chosen for use in the analytical model by simply changing the power parameter of the rule. The final slope of the implied bilinear rule is taken to be the same as that of the Ramberg-Osgood rule when the displacement is infinity. This is not the same as the bilinear rule usually used by designers. The more usual design bilinear rule is generated by requiring that the area under the experimental hysteretic loops for the bearings be the same as the that obtained from the test data. This gives a different initial slope than the implied bilinear rule associated with the Ramberg-Osgood relationship. It should be noted that a “design” bilinear rule can be constructed from the generalized Ramberg-Osgood rule once it has been obtained from the quick release field data.

SECTION 7

REFERENCES

AASHTO (1991), "Standard Specification for Highway Bridges", American Association for State Highway and Transportation Officials(AASHTO), 15th edition, 1989 and Interim Specification 1990, 1991.

Aiken, Ian D., James M. Kelly, and Frederick, F. Tajirian, 1989, "Mechanics of low shape factor elastomeric seismic isolation bearings", Report NO. UCB/EERC-89/13, Earthquake Engineering Research Center, University of California at Berkeley.

Asher, J. W., S. N. Hoskere, R. D. Ewing, R. L. Mayes, M. R. Button, and D. R. Van Volkinburg, (1997). "Performance of Seismically Isolated Structures in the 1994 Northridge and 1995 Kobe Earthquakes", Building to Last, Leon Kempner, Jr. and Colin B. Brown, Editors, Proceedings of Structures Congress XV, Published by ASCE, pp. 1128-1132.

Buckle, I. G., Ronald, L. Mayes, R. L., (1990) "Seismic Isolation: History, Application, and Performance - A world View", Earthquake Spectra, Vol. 6, No. 2, pp 161-201, 1990.

Chen S. S., J. B. Mander, D. S. MacEwan, and B. Mahmoodzadegan, 1993, "Quick-Release Behavior of Two Eastern U.S. Highway bridges", Proceedings of the 10th International Bridge Conference, Pittsburgh, Pa., June 1993.

Clough R. W. and J. Penzien, "Dynamics of Structures", Second edition, Chapter 8, McGraw-Hill Inc., 1975.

Desai, C. S. and Wu T. H., (1976), "A general function for stress-strain curves", Proc 2nd Int. Conf. For Numerical Methods in Geomech., Blacksburg, Va.

Douglas B. M., Maragakis, E. A., and Nath B., (1990) , "Static Deformation of Bridges from Quick-Release Dynamic Experiments," J. of Struct. Engin., Proceedings of ASCE, Vol. 116, No. 8 00.2201-2213.

Dynamic Isolation System, Inc., "AASHTO Design Procedures For Seismically Isolated Bridges", March 1992.

Gilani, A. S., Mahin, S. A., Fenves, G. L., Aiken, I. D., and Chavez, J. W., "Field Testing of Bridge Design and Retrofit Concept, Part 1 of 2: Field Testing and Computer Analysis of a Four-Span Seismically Isolated Viaduct in Walnut Creek, California," Reprot No. UCB/EERC-95/14, Earthquake Engineering Research Center, University of California at Berkeley, Berkeley, California, December 1995.

Hibbeler, "Structural Analysis", Third edition, 1992.

Hooke R. And T. A. Jeeves, (1961), "Direct Search solution of Numerical and Statistical Problem", J. Assoc. Comp. Mach., Vol. 8, pp. 212-229.

Kelly, J. M., and Hodder S. B., (1981) "Experimental Study of Lead and Elastometric Dampers for Base Isolation System", Report of National Science Foundation, Earthquake Engineering Research Center, University of California, Berkeley, CA, Report No. UCB/EERC-81/16.

Kelly, James, M., Ian G. Buckle, and Chan Ghee Koh, 1987, "Mechanical characteristics of base isolation bearings for a bridge deck model test", Report NO. UCB/EERC-86/11, Earthquake Engineering Research Center, University of California at Berkeley.

Kelly, J. M., 1990, "Base Isolation: Linear Theory and Design", Earthquake Spectra, Vol. 6, No. 2, 1990.

King G. 1980, "Mechanical energy dissipation for seismic structures", Rep. 228, Dept. Of Civil Eng., Univ. Of Auckland, New Zealand.

Mayes, R. L., Buckle, L. G., Kelly, T. E., and Lindsay, R. J., (1992), "AASHTO Seismic Isolation Design Requirements for Highway Bridges", Structures Congress, p 656-659, March 1992.

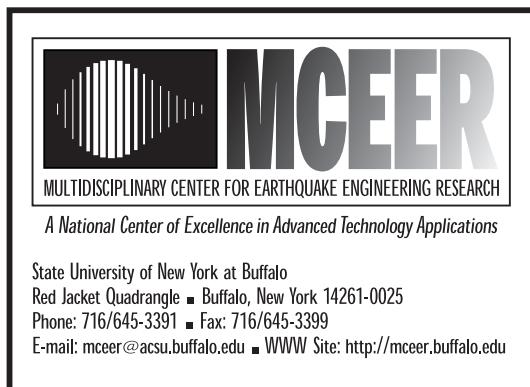
McKay, G. R., H. E. Chapman, and D. K. Kirkcaldie, (1990). "Seismic Isolation: New Zealand Applications", Earthquake Spectra, Vol. 6, No. 2, pp 203-221, 1990.

Moehle, J. P., (1994). "Preliminary Report on the Seismological and Engineering Aspects of January 17, 1994 Northridge Earthquake." Rep. No. UCB/EERC-94/01, Jan. 1994, Earthquake Engineering Research Center, Richmond, California.

Spiridon Vrontinos, (1994). "Analytical and experimental studies on the seismic response of short span reinforced concrete bridges", Thesis (Ph. D.), University of Nevada, Reno, 1994

Wendichansky, D. A., S. S. Chen, and J. B. Mander, (1995). "In-Situ Performance of Rubber Bearing Retrofits". National Seismic Conference on Bridges and Highways. San Diego, California, December, 1995.

Wendichansky, Daniel A. 1996, "Experimental Investigation of the Dynamic Response of Two Bridges Before and After Retrofitting with Elastometric Bearings", PhD Dissertation, Civil Engineering Department, University of New York at Buffalo.



ISSN 1520-295X